


## RESEARCH ARTICLE

# Adjustment of measurement errors to reconcile precipitation distribution in the high-altitude Indus basin

Zakir Hussain Dahri<sup>1,2</sup>  | Eddy Moors<sup>3,4</sup> | Fulco Ludwig<sup>1</sup> | Shakil Ahmad<sup>5</sup> | Asif Khan<sup>6</sup> | Irfan Ali<sup>7</sup> | Pavel Kabat<sup>1,8</sup>

<sup>1</sup>Water Systems and Global Change, Wageningen University and Research, Wageningen, The Netherlands

<sup>2</sup>Climate Energy and Water Resources Institute, National Agricultural Research Centre, Pakistan Agricultural Research Council, Islamabad, Pakistan

<sup>3</sup>IHE Delft Institute for Water Education, Delft, The Netherlands

<sup>4</sup>Earth and Climate Cluster, Faculty of Earth and Life Sciences, VU University Amsterdam, Amsterdam, The Netherlands

<sup>5</sup>NUST Institute of Civil Engineering, National University of Science and Technology, Islamabad, Pakistan

<sup>6</sup>Department of Civil Engineering, University of Engineering and Technology, Peshawar, Pakistan

<sup>7</sup>Natural Resources Division, Pakistan Agricultural Research Council, Islamabad, Pakistan

<sup>8</sup>International Institute for Applied Systems Analysis, Laxenburg, Austria

**Correspondence**

Z. H. Dahri, Water Systems and Global Change, Wageningen University and Research, Wageningen, The Netherlands.

Email: zakir.dahri@wur.nl; zakirdahri@yahoo.com

**Funding information**

Netherlands Organization for International Cooperation in Higher Education through Netherlands Fellowship Program, Grant/Award Number: NFP-PhD.11/ 898; Netherlands Organization for Scientific Research through Young Scientists Summer Program; International Development Research Centre; Department for International Development, UK Government

Precipitation in the high-altitude Indus basin governs its renewable water resources affecting water, energy and food securities. However, reliable estimates of precipitation climatology and associated hydrological implications are seriously constrained by the quality of observed data. As such, quantitative and spatio-temporal distributions of precipitation estimated by previous studies in the study area are highly contrasting and uncertain. Generally, scarcity and biased distribution of observed data at the higher altitudes and measurement errors in precipitation observations are the primary causes of such uncertainties. In this study, we integrated precipitation data of 307 observatories with the net snow accumulations estimated through mass balance studies at 21 major glacier zones. Precipitation observations are adjusted for measurement errors using the guidelines and standard methods developed under the WMO's international precipitation measurement intercomparisons, while net snow accumulations are adjusted for ablation losses using standard ablation gradients. The results showed more significant increases in precipitation of individual stations located at higher altitudes during winter months, which are consistent with previous studies. Spatial interpolation of unadjusted precipitation observations and net snow accumulations at monthly scale indicated significant improvements in the quantitative and spatio-temporal distribution of precipitation over the unadjusted case and previous studies. Adjustment of river flows revealed only a marginal contribution of net glacier mass balance to river flows. The adjusted precipitation estimates are more consistent with the corresponding adjusted river flows. The study recognized that the higher river flows than the corresponding precipitation estimates by the previous studies are mainly due to underestimated precipitation. The results can be useful for water balance studies and bias correction of gridded precipitation products for the study area.

**KEYWORDS**

bias correction of precipitation, high-altitude Indus basin, net mass balance contribution to river run-off, net snow accumulation adjustments, precipitation distribution, precipitation measurement errors

## 1 | INTRODUCTION

High mountain ranges around the world are important sources of freshwater storage and subsequent supplies to

downstream areas. Indus basin contains one of the most diversified and complex mountain terrains in the world. Precipitation in its high-altitude areas governs the renewable water resources determining water, energy and food

This is an open access article under the terms of the Creative Commons Attribution License, which permits use, distribution and reproduction in any medium, provided the original work is properly cited.

© 2018 The Authors. International Journal of Climatology published by John Wiley & Sons Ltd on behalf of the Royal Meteorological Society.

securities in the region. Run-off regime of the basin is predominantly controlled by winter- and summer-monsoon precipitations and summer temperatures (Yu et al., 2013). Yet, there is limited understanding and reliable evidence of quantitative and spatio-temporal distribution of the key climatic variables, particularly the precipitation (Hewitt, 2005; Immerzeel, Wanders, Lutz, Shea, & Bierkens, 2015; Mishra, 2015; Ragetti & Pellicciotti, 2012; Winiger, Gumpert, & Yamout, 2005) leading to a large uncertainty in the hydro-climatic predictability in the basin (Lutz, Immerzeel, Kraaijenbrink, Shrestha, & Bierkens, 2016). Overall scarcity and biased spatial and altitudinal distribution of the in situ observations are the primary reasons for this uncertainty and knowledge gap. Substantial increase in research on glacio-hydro-climatology of the Hindukush–Karakoram–Himalayan (HKH) region is observed since the International Panel on Climate Change (IPCC) released its fourth assessment report, which claimed that “glaciers in Himalayas are receding faster than in any other part of the world and, if the present rate continues, the likelihood of their disappearing by the year 2035 is very high” (Cruz et al., 2007). Later, IPCC withdrew this statement due to an inaccurate citation of the grey literature. Yet, most of the subsequent research is mainly focused on improved methods using more or less the same commonly available data sets that use low altitude and largely unrepresentative observations in the development or validation of these data sets.

Adequate monitoring of climatic variables to better represent the entire range of a diverse climate of this complex mountain terrain is essential for reducing uncertainties and inferring informed policy decisions. However, such an observational network in the study region is lacking mainly due to resource constraints and logistical limitations. To overcome the observational data gaps, the hydro-climatologists generally rely on numerous global/regional-scale gridded products derived through various means (e.g., climate models reanalysis, merged model and station observations, merged satellite estimates and station observations, and derived solely from station observations). However, the strong gradients and extreme heterogeneity of this complex mountain terrain are inadequately captured by the gridded products due to their coarse resolution and use of non-representative climate data in their development or validation (Dahri et al., 2016; Immerzeel et al., 2015; Reggiani & Rientjes, 2015). As such, the precipitation estimates by a number of earlier studies (e.g., Akhtar, Ahmad, & Booij, 2008; Bocchiola et al., 2011; Bookhagen & Burbank, 2010; Central Water Commission and National Remote Sensing Centre, 2014; Immerzeel, Droogers, de Jong, Bierkens, 2009, 2010; Immerzeel, Pellicciotti, & Shrestha, 2012; Lutz, Immerzeel, & Kraaijenbrink, 2014; Lutz, Immerzeel, Shrestha, & Bierkens, 2014; Mukhopadhyay, 2012; Reggiani & Rientjes, 2015; Tahir, Chevallier, Arnaud, & Ahmad, 2011) that used the gridded

data sets show highly contrasting but consistently underestimated precipitation in most parts of the high-altitude Indus basin.

Numerous efforts to accurately estimate precipitation in this region only partially succeeded due to lack of observed data but significantly underlined the relevance and severity of the problem. In many hydrological modelling studies, the underestimated precipitation is often compensated for with other parameters like evapotranspiration and/or snow/glacier melt factors (Lutz, Immerzeel, Shrestha, & Bierkens, 2014; Pellicciotti, Buergi, Immerzeel, Konz, & Shrestha, 2012; Schaepli, Hingray, Niggli, & Musy, 2005). This results in inaccurate and suboptimal inferences regarding precipitation distribution, snow/glacier cover dynamics and associated melt water contributions. Adam, Clark, Lettenmaier, and Wood (2006) used a water balance approach to indirectly correct monthly precipitation in mountain regions from an existing global data set and provided reasonable approximations at basin level. However due to inaccuracies in water balance components and use of biased gridded data sets developed from limited observations, their results show large differences in precipitation amounts and distribution patterns at sub-basin scale in the study area. For example, precipitation in the high-mountain Karakorum region is largely underestimated due to lack of stations in this area, whereas higher precipitation amounts are shown for the southern parts of western Himalayan region that hosts many precipitation gauges. Lutz, Immerzeel, Shrestha, and Bierkens (2014) recognized underestimation of APHRODITE precipitation and multiplied it with an arbitrary constant factor of 1.17 to account for the inherent underestimations.

Recently, Immerzeel et al. (2015) and Dahri et al. (2016) used other sources of data/information to cover the observational gaps and provided relatively better estimates of precipitation amounts and distribution in the high-altitude Indus basin. The approach adopted by Immerzeel et al. (2015) used the glacier mass balance (GMB) estimates of Kääb, Berthier, Christopher, Gardelle, and Arnaud (2012) to inversely infer the high-altitude precipitation. Using APHRODITE as the basis, they computed vertical precipitation gradients until observed mass balance matched the simulated mass balance for the 550 major glacier systems in the Indus basin. However, precipitation in the basin does not have constant and linear gradients (Dahri et al., 2016), APHRODITE precipitation distribution is highly biased (Dahri et al., 2016; Palazzi, von Hardenberg, & Provenzale, 2013) and their mass balance computations are uncertain due to the use of extremely elusive direct evapotranspiration losses and negligence of percolation, interception and sublimation losses from the precipitation. Moreover, precipitation estimates of Immerzeel et al. (2015) might be affected by the overestimated basin boundaries of Shyok and Indus at Tabela sub-basins. However, Dahri et al. (2016) integrated the available station observations with the indirect precipitation estimates at the

accumulation zones of major glacier systems. They employed Kriging with external drift (KED) interpolation scheme with elevation as predictor to derive the spatio-temporal distribution of mean monthly and annual precipitation climatologies. They validated their precipitation estimates by the individual station observations and the observed specific run-off at sub-basin scale. However, if the net mass balance (i.e., slightly negative as estimated by Käähb et al., 2012) and precipitation losses (direct evapotranspiration, percolation, interception and sublimation) in the basin are taken into account, the Dahri et al. (2016) estimates still seem to be on lower side. The underestimated precipitation relative to the corresponding specific run-off in most sub-basins may be attributed to three possible reasons: (a) overestimated river flows, (b) significant contribution of snow/glacier melt without an adequate amount of precipitation to feed/sustain the glacier systems and (c) underestimated precipitation. Given the technological advancements and relative precision of discharge measurement techniques and quality control ensured by the data collecting agencies, river flows are generally considered to be adequately accurate. However, there is considerable speculation but little analysis and evidence regarding the contribution of net glacier mass imbalance to the river flows. Although Immerzeel et al. (2015) attributed the observed gap between precipitation and streamflow to the underestimated precipitation rather than the observed GMB, there is an emergent need to quantify the contribution of net glacier mass imbalance to the river flows. The underestimated precipitation by Dahri et al. (2016) is probably due to the use of net precipitation estimates from the glacier accumulation zones and the raw/uncorrected precipitation gauge observations which are subject to significant measurements errors (Chen et al., 2015; Goodison, Louie, & Yang, 1998; Legates, 1987; Legates & Willmott, 1990; Sevruk & Hamon, 1984; Wolff, Isaksen, Petersen-Øverleir, Ødemark, & Reitan, 2015).

The IPCC in its fifth assessment report stressed the need for adjustment of precipitation measurement errors and declared that observational uncertainties in precipitation may limit the confidence in the assessment of climatic change impacts (Bindoff et al., 2013). The measurement errors in precipitation observations, particularly the wind-induced undercatch of solid precipitation in windy conditions can be substantial (Adam & Lettenmaier, 2003; Kochendorfer et al., 2017a, 2017b; Wolff et al., 2015). This is particularly important in the high-altitude Indus basin where moderately strong winds are a common phenomenon; temperature mostly remains below the freezing point and the majority of precipitation falls in the form of snow. Legates (1987), Legates and Willmott (1990) and Adam and Lettenmaier (2003) adjusted the systematic biases of global precipitation products including the Indus basin but these data sets included only a few stations located in relatively dry valleys in the study area. The uncertainties in precipitation estimates may significantly affect the outcomes of hydrological/land surface models and mass

balance studies. A systematic error of over 3% in rainfall measurement could lead to substantial underestimation of water in the hydrologic system (e.g., Biemans et al., 2009; Sevruk, 1982). Therefore, the systematic errors in precipitation observations must be corrected if the measurements are to be used for climate change, hydrological modelling and water balance studies (Legates & Willmott, 1990; Voisin, Wood, & Lettenmaier, 2008; Wolff et al., 2015). This study attempts to address the above concerns by adjustment of the systematic measurement errors in precipitation observations, adjustment of net snow accumulation for the ablation losses and adjustment of river flows for the net mass balance contributions. The ultimate goal of this research is to facilitate creation of an accurate and consistent gridded precipitation product for the highly under-explored region of Indus basin. The results will have considerable implications for water resources planning and management in both upstream (high altitude) and downstream (low altitude) areas of the Indus basin.

## 2 | STUDY AREA

The study area covers the high-altitude catchments of the Indus river, which originates from the Tibetan Plateau (TP) and the HKH mountain regions (Figure 1). The total area of the study region is about  $4.03 \times 10^5$  km<sup>2</sup> of which 50% is above 4,000 m a.s.l. and another 24% between 2,500 and 4,000 m a.s.l. Precipitation in the study area is influenced by multiple weather systems. The Indian summer monsoon brings moisture from the Indian Ocean and Bay of Bengal and is the dominant system in the southeastern areas. The western disturbances originating from the Mediterranean and Caspian Sea dominate the southwestern and northwestern areas bringing winter monsoon during December–April months. During spring and early summer, irregular collapses of the Tibetan anticyclone sometimes allow monsoonal air masses to penetrate into the Karakoram Range (Wake, 1989). Direct transport of moisture from the Arabian Sea and local evapotranspiration also have considerable influence as about 5–40% of the precipitation falling in the Himalayas originates from the irrigated areas in northern India and Pakistan (Harding, Blyth, Tuinenburg, & Wiltshire, 2013; Tuinenburg, Hutjes, & Kabat, 2012; Wei, Dirmeyer, Wisser, Bosilovich, & Mocko, 2013). However, the hydrological cycle in the study region is usually intensified when all or some of these systems interact with each other.

## 3 | DATA AND METHODS

### 3.1 | Precipitation observations

Indus is a transboundary river basin, as such its meteorological data are scattered in four countries (i.e., Afghanistan, China, India and Pakistan). The meteorological data of

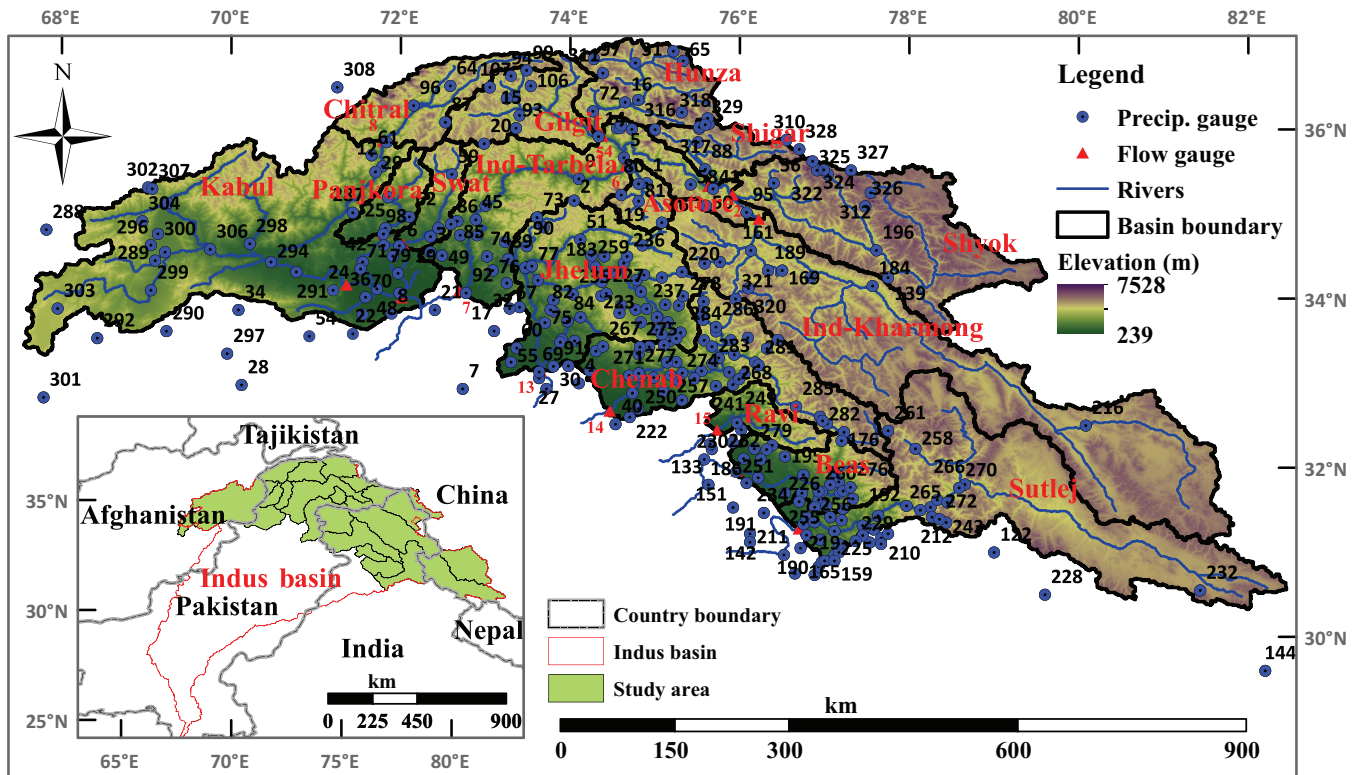


**FIGURE 1** Location of study area (bottom) and description of sub-basins, river network and location of precipitation and flow measuring gauges (top). The red triangle and associated numbers refer to flow measuring gauges on various tributaries, which are (a) Indus at Kharmoning, (b) Shyok at Yogo, (c) Shigar at Shigar, (d) Hunza at Dainyor, (e) Gilgit at Gilgit, (f) Astore at Doyian, (g) Indus at Tarbela dam, (h) Chitral at Chitral, (i) Panjgora at Zulum Br., (j) upper swat at Chakdara, (k) Kabul at Warsak, (l) Kabul at Nowshera, (m) Jhelum at Mangla dam, (n) Chenab at Marala, (o) Ravi at Thein dam, (p) Beas at Pong dam and (q) Sutlej at Bhakra dam. The blue circles and associated numbers refer to the precipitation gauges, details of which are given at Table S1 [Colour figure can be viewed at [wileyonlinelibrary.com](http://wileyonlinelibrary.com)]

Pakistani parts were collected from Pakistan Meteorological Department (PMD) and Pakistan Water and Power Development Authority (WAPDA). Precipitation data of the station located in Afghanistan are available with Afghan-Agriculture UCDAVIS (<http://afghanag.ucdavis.edu/natural-resource-management/weather>), NOAA Central Library of US ([https://docs.lib.noaa.gov/rescue/data\\_rescue\\_afghanistan.html](https://docs.lib.noaa.gov/rescue/data_rescue_afghanistan.html)) and US Geological Survey (<http://edcintl.cr.usgs.gov/downloads/sciweb1/shared/afghan/downloads/documents/>), while precipitation data of Indian and a couple of Chinese stations were downloaded from KNMI Climate Explorer (<https://climexp.knmi.nl>). In addition, we derived monthly precipitation data of many stations from Winiger et al. (2005), Mieke, Winiger, Bohner, & Yili (2001), Mieke, Cramer, Jacobsen, and Winiger (1996), Eberhardt, Dickore, and Mieke (2007), Arora, Singh, Goel, and Singh (2006), Singh and Kumar (1997) and Singh, Ramasastri, and Kumar (1995).

Information regarding the gauge type, use of wind shield if any, orifice area and height of the gauge orifice were taken from Sevruck and Klemm (1989) and Bureau of Indian Standards (1992a, 1992b) and from PMD and WAPDA through personal communications. Until 1969, the most extensively used rain gauge in India was non-recording (Symon's gauge or MK2 model) with orifice area

of 127 cm<sup>2</sup> and instrument height of 0.3 m (Sevruck & Klemm, 1989). Thereafter, Indian standards adopted by the Bureau of Indian Standards (BIS) for design and manufacturing of meteorological instruments are strictly followed and Indian rain gauge (20-22-P) reinforced with fibreglass polyester is predominantly used (Bureau of Indian Standards, 1992a, 1992b). Similarly, the most widely used rain gauge type by PMD has been non-recording MK2 (13-15-C) model with orifice area of 127 cm<sup>2</sup> and instrument height of 0.3 m. In 2010, PMD started using its own model, which is tipping bucket rain gauge (TBRG) type equipped with logger and standalone method of monitoring rainfall, with 0.2 mm (moderate rain) tipping bucket, orifice area of 400 cm<sup>2</sup> and gauge height of 0.6 m. WAPDA uses both automatic weighing and standard meteorological service manual rain gauges. The automatic gauges have an orifice area of 127 cm<sup>2</sup>, tipping capacity of 0.254 mm and gauge height of 0.3 m (Water and Power Development Authority, 2003). A manual gauge is read in conjunction with each automatic gauge as a check on the total rainfall. In 1994–95, WAPDA installed 20 automatic data collection platforms (DCPs) in the high-altitude areas that use snow pillows to measure both solid and liquid precipitation as water equivalent (SIHP, 1997). The observatories installed and maintained by the University of Bonn under the CAK

program used the automatic weather stations including data logger, tipping bucket and snow depth gauge to measure precipitation (Miehe, Cramer, et al., 1996). Afghanistan mainly uses the Tretyakov (20-24-G) type of rain gauge without windshield having orifice area of 200 cm<sup>2</sup> and 0.4 m height (Sevruk & Klemm, 1989). The metadata of 305 precipitation observatories and 21 glacier observation points used in this study are outlined and described in Table S1, Supporting information).

### 3.2 | Temperature and wind speed observations

The adjustments for wind-induced under-catch of precipitation observations require corresponding data of temperature and wind speed. However, out of 324 stations, temperature data were available for only 114 stations (Table S1). We therefore derived monthly lapse rates based on elevation and latitude and estimated the maximum and minimum temperatures for the remaining stations. The observed data of wind speed was available for only 25 stations. Wind speed for the remaining stations is taken from the Japanese 55-year Reanalysis (JRA55) data set (Kobayashi et al., 2015). JRA55 provides wind speed estimates at the standard anemometer height of 10 m, whereas the station-based observed wind speed is measured at 2 m height. In order to get an idea of the accuracy of the JRA55 wind speed data, we compared it with the observed wind speed for the 25 stations. For this purpose, we computed wind speed from the U- and V-components at 10 m height and downscaled it to match the 2 m height of stations using the Monin Obukhov theory (Businger & Yaglom, 1971; Obukhov, 1971). Although we could not detect large differences and/or any definite and strong trends, a tendency of slightly underestimated wind speed in low-altitude areas and vice versa in high-altitude areas is noticed. We also observed marginally increased wind speeds during November–February months and slightly decreased wind speeds during March–October months for the JRA55 data. Due to insufficient observed data of wind speed, we have neglected these minor differences and used wind speed data of JRA55 as such. Nevertheless, such minor differences of wind speeds in JRA55 data might result in slight overestimation of precipitation adjustments in the higher-altitude areas during four (November–February) winter months and slight underestimation of precipitation adjustments in the lower-altitude areas during the remaining months.

### 3.3 | River flows

Daily data of the observed river flows at sub-basin level for 14 hydrological stations (Figure 1) in the study area were collected from WAPDA. We used flow data of Jhelum and Chenab rivers for 1961–1970 period and all the rivers in the western part sub-basins for 1999–2011 period to coincide with the precipitation data periods. Ravi, Beas and Sutlej

basins are located in India and their inflow data are not publicly available. Therefore, we extracted mean monthly river flows from Adeloje, Remesan, and Soundharajan (2016) for the Beas River at Pong dam for 2000–2008 period and from Asian Development Bank (2010) for the Sutlej River at Bhakra dam for 1962–1971 period. The river discharge data for the Ravi at Mukesar (near Thein dam) is collected from the global river discharge database (RivDIS v1.1) for the period of 1968–1979. It is worth to note that there are considerable diversions in some sub-basins on the upstream side of their rim stations (e.g., at Warsak, Nowshera and Tarbela), which are often overlooked by previous studies. We also collected the data of these upstream diversions and added them to the flows of the respective sub-basins. River flow data of coinciding time periods are used to validate the adjusted precipitation at sub-basin scale.

### 3.4 | Precipitation measurement error adjustment methods

The amount of actual precipitation reaching the ground is generally higher than what is measured in precipitation gauges due to measurement errors, which usually depend on the form of precipitation, gauge type, topography, vegetation around the gauge site and the exposure of the gauges to prevailing temperatures and winds. Wind-induced under-catch is by far the most dominant source of errors in gauge-measured precipitation observations (Adam & Lettenmaier, 2003; Goodison et al., 1998; Michelson, 2004; Wolff et al., 2015), yet most of the widely used global precipitation data sets are not adjusted for such errors (Adam & Lettenmaier, 2003). While recognizing the significance of measurement errors in precipitation observations, the World Meteorological Organization (WMO) initiated a comprehensive program of international precipitation measurement intercomparisons during 1960–1993 and established the pit gauge (Sevruk & Hamon, 1984) and the double-fence international reference (DFIR) (Goodison et al., 1998) as the standard reference gauges for liquid (rain) and solid (snow) precipitation, respectively. Sevruk and Hamon (1984) and Goodison et al. (1998) also underlined the need for gauge calibration and adjustment of errors to increase reliability of the precipitation data. However, the agencies involved in measurement of precipitation in the Indus basin generally indicate to follow the WMO standards for design, construction, installation and operation of precipitation gauges but hardly or inadequately adjust the systematic measurement errors at the source, which signifies the need for correction of measurement errors.

Sevruk (1982) related and statistically analysed various components of the systematic measurement errors to the meteorological and instrumental factors and proposed a general equation for adjustment of gauge-measured precipitation errors. Legates (1987) later modified it to account for

both liquid and solid precipitation components separately. The modified equation is expressed as

$$P_a = (1 - R)K_r(P_m + \Delta P_{wr} + \Delta P_{tr} + \Delta P_{er}) + RK_s(P_m + \Delta P_{ws} + \Delta P_{ts} + \Delta P_{es}), \quad (1)$$

where  $P_a$  is adjusted precipitation (mm),  $R$  is proportion of solid precipitation,  $K$  is correction coefficient that accounts for wind-induced losses,  $P_m$  is measured precipitation (mm),  $\Delta P_w$  is wetting losses (mm),  $\Delta P_e$  is evaporation losses (mm),  $\Delta P_t$  is trace precipitation (mm) and subscripts  $r$  and  $s$  denote rain and snow components, respectively. Legates (1987) model was developed for a variety of manual rain gauges including Nipher, Tretyakov and MK1/MK2 models with and without windshields. However, significant uncertainties remained for wind-induced under-catch of solid precipitation particularly by automatic precipitation gauges. Nitu and Wong (2010) observed much larger variation between gauges and windshield configurations for automatic stations than for manual stations.

Wolff et al. (2015) compared precipitation data from the standard automatic Geonor precipitation gauge with data from a reference configuration consisting of an automatic precipitation gauge (Geonor T200-BM) and an Alter wind shield with double-fence construction. They derived an adjustment model to determine catch efficiency as a continuous function of both wind speed and air temperature using Bayesian statistics to more objectively choose the model that best describes the data. Wolff's model allows solid precipitation adjustments at wind speeds greater than 7.0 m/s. However, it is also gauge/shield-specific and different site specificities and gauge/shield configurations might result in different adjustment functions.

Kochendorfer et al. (2017a) analysed precipitation measurements from eight different WMO-SPICE sites for both unshielded and single-Alter-shielded OTT Pluvio<sup>2</sup> and Geonor T-200B3 types of weighing gauges. They grouped unshielded and single-Alter-shielded precipitation gauge configurations separately irrespective of gauge types and created a single transfer function of air temperature and wind speed using the corresponding measurements from the reference gauge. They also derived the coefficient fits for both unshielded and single-Alter-shielded precipitation gauges at gauge height as well as 10 m height. The derived transfer function is expressed as

$$CE = e^{-a(U)}(1 - \text{TAN}^{-1}(b(T_{\text{air}}) + c)), \quad (2)$$

where  $T_{\text{air}}$  is mean air temperature ( $^{\circ}\text{C}$ ),  $U$  is wind speed (m/s),  $a$ ,  $b$  and  $c$  are the coefficients fit to the data and  $\text{TAN}^{-1}$  is the inverse of tangent function.

Our method of adjusting systematic errors in precipitation measurements largely follows the approach by Adam and Lettenmaier (2003) using the "liquid" part of the model by Legates (1987) and uses the model by Kochendorfer et al. (2017a) for adjustment of the solid precipitation

component. The detailed methods for computation of the required variables in Equation (1) are described in the supplement available on-line. The coefficient values in Equation (2) ( $a = 0.0623$ ,  $b = 0.776$ ,  $c = 0.431$ ) are taken as determined at 10 m height by Kochendorfer et al. (2017a). We used the coefficient values of 10 m height because most of our wind speed data belonged to the JRA55 data set, which provides wind speed data at 10 m height. The observed wind speed at 25 stations is converted from observation height to 10 m height using the Monin Obukhov theory (Businger & Yaglom, 1971; Obukhov, 1971).

### 3.5 | Adjustment of net snow accumulations

The meteorological stations in the study area are unevenly distributed in both horizontal and vertical direction. Scarcity of precipitation measurements at higher-altitude areas, where the bulk of precipitation falls, seriously limits an accurate assessment of precipitation climatology and its hydrological implications. In order to overcome this observational data gap, we assumed 21 virtual stations at the major glaciers where the net snow accumulations were estimated through mass balance studies using snow pillows, snow pits and ice cores (e.g., Batura Investigations Group, 1979; Bhutiyan, 1999; Decheng, 1978; Hewitt, 2011; Kick, 1980; Mayer et al., 2014; Mayer, Lambrecht, Belò, Smiraglia, and Diolaiuti (2006); Mayewski, Lyons, & Ahmad, 1983; Mayewski, Lyons, Ahmad, Smith, & Pourchet, 1984; Qazi, 1973; Shroder, Bishop, Copland, & Sloan, 2000; Wake, 1989). However, most of these mass balance studies were undertaken in the active ablation zones of the glaciers, where ablation and accumulation processes are happening simultaneously. Generally, glacier ablation is the function of ablation rate, altitude of the equilibrium line altitude (ELA) and the elevation difference between mean ELA and the glacier observation point. Ablation zones are the areas below the ELA, which is the elevation at which the annual net mass of the glacier remains zero and the area above this elevation is known as the accumulation zone (Cuffey & Paterson, 2010). Hence, the estimated net glacier mass accumulations are subject to ablation losses until the next accumulation period. The ablation gradients can be variable depending on debris cover and surface albedo or energy availability to melt the exposed glaciers. Wagnon et al. (2007) observed ablation gradients of 0.60–0.81 m w.e. (water equivalent) for each 100 m with a mean value of 0.69 m w.e. over a period of 4 years of mass balance studies at the Chhota Shigri glacier, western Himalaya. Yu et al. (2013), based on glacier studies by Mayer, Lambrecht, et al. (2006) and Wagnon et al. (2007) in the Karakoram and western Himalaya, assumed an ablation gradient of 1 m w.e. per 100 m for the upper Indus basin. Hewitt, Wake, Young, and David (1989) however, estimated an ablation gradient of 0.5 m per 100 m for the middle portion of the ablation zone on the Biafo glacier in the central part of the

Karakoram. No ablation above ELA is assumed. We selected the rather conservative estimates of ablation gradient by Hewitt et al. (1989) and adjusted the net accumulations by taking the ELA as the boundary for the ablation process. However, the location of ELA can vary from location to location. In temperate glaciers, usually the snow line elevation (SLE) and ELA are often assumed to be the same. The estimates for mean ELA at sub-basin scale are taken from Khan, Naz, and Bowling (2015), who estimated ELA values based on SLE.

### 3.6 | River flow adjustments

WAPDA uses standard flow measuring devices to ensure high quality river flow data. The primary river flow measuring technique uses area velocity measurements to determine the stage–discharge relationships and associated rating tables. The results are verified by area-velocity method, area-slope method, contracted opening measurements, or computation of flow over dams or weirs (Water and Power Development Authority, 2012). The daily mean discharge values are computed from the mean gauge heights and corresponding calibrated rating tables. In case of extremely high discharges, the rating curves are extrapolated by applying simple linear regression between the gauge height and discharge measurements. The actual measurements are however taken 4–8 times per month. The intermediate daily values are estimated from the rating tables. The accuracy of stream flow measurements depends primarily on stability of the stage–discharge relationship, frequency of discharge measurements if the relationship is unstable, and accuracy in the observation of the stage and measurement of discharges. In general, monthly and annual mean values are more accurate than daily values because of compensation of random errors. WAPDA evaluates the probable accuracy of discharge measurements as excellent (error < 5%), good (error < 10%), fair (error < 15%) and poor (error > 15%). In general, a probable accuracy of 0–5% is aimed for.

Although river flow data may still be subject to some degree of uncertainty due to measurement errors, we assumed river flows as adequately accurate considering the relative precision of discharge measurement techniques and quality control ensured by the data collection agencies.

To account for the contribution of net glacier mass imbalance in each sub-hydrological basin, we adjusted the measured river flows. Kääh et al. (2012) used satellite laser altimetry and a global elevation model and observed a slightly negative mass balance of  $-0.21 \pm 0.05$  m/year w.e. for HKH region during 2003–2008 with maximum rates of  $-0.66 \pm 0.09$  m/year w.e. in the western Himalayan (Jammu–Kashmir) areas. We derived the specific net mass balance rates at sub-basin scale from the mass balance estimates of Kääh et al. (2012) and took glacier areas from the Randolph Glacier Inventory (RGI) version 5.0 (Arendt et al., 2015) to compute the contribution of the changes in

the net glacial mass imbalance to the observed river flows. The adjusted river flows are used for validation of the adjusted precipitation estimates at sub-basin scale.

### 3.7 | Spatial interpolation

The actual and error-adjusted point measurements of mean monthly precipitation are spatially interpolated following Dahri et al. (2016), who used the KED interpolation scheme (Schabenberger & Gotway, 2005) with elevation as a predictor to derive spatio-temporal distribution of precipitation in the high-altitude Indus basin. The KED model includes a component of spatial autocorrelation and a component for multi-linear dependence on pre-defined variables (predictors). It considers the observations ( $Y$ ) at sample locations ( $s$ ) as a random variable of the form (e.g., Diggle & Ribeiro, 2007),

$$Y(s) = \mu(s) + Z(s), \quad (3)$$

$$\mu(s) = \beta_0 + \sum_{k=1}^K \beta_k \cdot x_k(s), \quad (4)$$

where  $\mu(s)$  describes the deterministic component of the model (external drift or trend) and is given as a linear combination of  $K$  predictor fields  $x_k(s)$  (trend variables) plus an intercept ( $\beta_0$ ). The  $\beta_k$  are denoted as trend coefficients, while  $Z(s)$  describes the stochastic part of the KED model and represents a random Gaussian field with a zero mean and a second-order stationary covariance structure. The latter is conveniently modelled by an eligible parametric semi-variogram function describing the dependence of semi-variance as a function of lag (possibly with a directional dependence). Dahri et al. (2016) provided a detailed account of the KED interpolation method including model description and functionalities, reasons for its selection and comparative advantages of its use in the high-altitude Indus basin.

### 3.8 | Cross validation of the adjusted precipitation

We used exactly the same approach of interpolation and cross validation as adopted by Dahri et al. (2016), where the cross validation applied on the observed and predicted values from all the stations is used to assess the errors/uncertainty associated with the interpolation scheme by using error scores of the relative bias ( $B$ ) and the relative mean root-transformed error ( $E$ ), which are defined as

$$B = \frac{\sum_{i=1}^n P_i}{\sum_{i=1}^n O_i}, \quad (5)$$

$$E = \frac{\frac{1}{n} \sum_{i=1}^n (\sqrt{P_i} - \sqrt{O_i})^2}{\frac{1}{n} \sum_{i=1}^n (\sqrt{O_i} - \sqrt{O_i})^2}, \quad (6)$$

where  $P_i$  and  $O_i$  are the predicted and observed precipitation values, respectively, while  $O$  is the average of all (or a

subset of) the station observations and  $n$  refers to the number of precipitation values.

Under ideal conditions, the overall performance of the employed regression models and interpolation estimates at basin/sub-basin scale can also be cross validated by applying the continuity equation suggested by Budyko (1974), which is given by

$$\frac{\Delta S}{\Delta t} = P - Q - ET - G, \quad (7)$$

where  $P$ ,  $Q$ ,  $ET$  and  $G$  are the basin-average precipitation, run-off, evapotranspiration and net groundwater discharge, respectively, while  $\Delta S$  is the net change in storage for a given time increment ( $\Delta t$ ). Equation (7) can be modified by adding interception ( $I$ ), sublimation ( $S$ ) and net mass balance ( $\Delta MB$ ) contributions for the highly glacierized and snowpack-dependent river basins as follows:

$$\frac{\Delta S}{\Delta t} = P - Q - ET - G - I - S + \Delta MB. \quad (8)$$

Unfortunately, there are no independent data sets of actual evapotranspiration, sublimation, interception and the net groundwater discharge for the study area. The global-scale data sets of these variables are generally more uncertain than precipitation itself; therefore, it would be unwise to validate the estimated precipitation with these extremely uncertain data sets. Nevertheless, surface storage and groundwater recharge are mostly very low in high-altitude areas, which are mostly rocky bare mountains with steep slopes and no groundwater. Precipitation may travel long distances through breaches but ultimately joins the river streams as base flow. Although there might be considerable delay effects, these may be considered negligible for long-term average conditions. Similarly, the surface storage due to topographical undulations may also have a delaying effect. Interception by the vegetation cover and sublimation (direct evaporation from the snow glacier fields) are included in the total direct evapotranspiration. Direct evapotranspiration is notoriously complex to measure as it is among others a function of water availability as well as water demand. The available global-scale gridded data sets of actual evapotranspiration are highly inconsistent in quantitative as well as spatial distribution terms and generally reflect overestimated values. We therefore rely mainly on the specific run-off and net mass balance data to validate our adjusted precipitation estimates.

## 4 | RESULTS

### 4.1 | Precipitation adjustments

To facilitate adjustment of measurement errors in precipitation observations, the corresponding air temperature is determined from elevation and latitude based lapse rates.

The results revealed a strong correlation of temperature with elevation and considerable correlation with latitude (Figures S2–S5). Significantly different gradients for each month and substantial difference among the gradients for maximum and minimum temperatures were observed (Table 1). Hence, use of a universally assumed or time-independent site-specific observed gradient of mean annual temperature to estimate maximum and minimum temperatures (e.g., Immerzeel, Pellicciotti, & Shrestha, 2012; Immerzeel, Van Beek, Konz, Shrestha, & Bierkens, 2012; Lutz, Immerzeel, Gobiet, Pellicciotti, & Bierkens, 2013) is probably not correct in the high-altitude Indus basin. Comparison of Table 1 and Figures S2 and S3 indicate that incorporation of latitude as an additional predictor improves the correlation of the regression models by up to 6.0% for maximum temperature and up to 1.5% for minimum temperature during 1999–2011. Almost similar trends are observed for 1961–1970 period. The contribution of elevation to the correction is positive in the summer months and negative in the winter months, while the contribution of latitude is positive throughout the year. The highest improvement is achieved during the monsoon season (July–September).

To illustrate the precipitation biases over the high-altitude Indus basin, the results for each individual station are presented. The applied bias adjustments significantly increased the gauge-measured precipitation. The highest increments are computed for wind-induced under-catch of solid precipitation followed by liquid precipitation under-catch, wetting losses and precipitation losses during trace events (Figure 2a–d). The solid precipitation under-catch generally dominates the higher-altitude stations, that is, elevations greater than 2000 m and during the December–April months. The range of liquid precipitation under-catch is much lower and mainly concentrates in the summer monsoon dominated low-altitude areas, that is, elevation less than 3,500 m. The wetting losses and unmeasured trace precipitation depend on the number of precipitation events. In many cases, particularly for the low-altitude stations experiencing lower wind speeds, the wetting losses exceeded the wind-induced under-catch of liquid precipitation due to the fact that it covers all the stations and both forms of precipitation (liquid and solid). The total bias between the gauge-measured and error-adjusted precipitation ranged from 12 to 773 mm/year for various individual stations and up to 1,000 mm/year for the glacier points (Figure 2e). The total absolute biases (corrections) for all the stations at monthly and annual scale are given at Table S2. The largest increases are found for the stations receiving greater precipitation amounts, located at higher-altitudes and encountering higher wind speeds. Based on the above mentioned corrections, we introduced monthly-scale correction factors (CFs) for each station (Table S3). These station based



CFs vary over space and time, with stronger magnitude in higher-altitude areas (Figure 2f) and during winter months (Table S3).

**TABLE 1** Multiple regressions for maximum and minimum temperatures for the western and eastern parts (Figure S1) covering the two time periods of 1999–2011 and 1961–1970, respectively.  $T_x$ 1-12 and  $T_n$ 1-12 refer to the calendar months for maximum and minimum temperatures, respectively.  $E$  denotes elevation (m) and  $L$  represents latitude (decimal degrees) of the meteorological stations.  $R^2$  is the combined correlation of temperature with  $E$  and  $L$

Regression equation for $T_x$	$R^2$ (%)	Regression equation for $T_n$	$R^2$ (%)
<i>1999–2011</i>			
$T_x1 = 31.5 - 0.00688E - 0.318L$	96.7	$T_n1 = 17.4 - 0.00534E - 0.307L$	91.1
$T_x2 = 38.1 - 0.00691E - 0.455L$	97.5	$T_n2 = 19.1 - 0.00559E - 0.285L$	92.3
$T_x3 = 41.3 - 0.00712E - 0.383L$	96.6	$T_n3 = 23.4 - 0.00567E - 0.278L$	93.8
$T_x4 = 44.5 - 0.00739E - 0.303L$	97.5	$T_n4 = 33.2 - 0.00567E - 0.428L$	94.1
$T_x5 = 41.0 - 0.00790E - 0.025L$	96.9	$T_n5 = 37.3 - 0.00599E - 0.404L$	94.5
$T_x6 = 19.1 - 0.00817E + 0.719L$	96.2	$T_n6 = 34.3 - 0.00591E - 0.220L$	95.6
$T_x7 = -9.47 - 0.00713E + 1.48L$	90.5	$T_n7 = 22.2 - 0.00575E + 0.166L$	95.4
$T_x8 = -5.13 - 0.00685E + 1.30L$	90.9	$T_n8 = 22.6 - 0.00567E + 0.136L$	95.5
$T_x9 = 8.60 - 0.00727E + 0.876L$	96.0	$T_n9 = 35.2 - 0.00532E - 0.341L$	95.1
$T_x10 = 20.4 - 0.00780E + 0.444L$	97.0	$T_n10 = 30.7 - 0.00518E - 0.380L$	91.8
$T_x11 = 39.0 - 0.00721E - 0.291L$	97.8	$T_n11 = 22.7 - 0.00515E - 0.300L$	90.3
$T_x12 = 38.8 - 0.00689E - 0.459L$	96.8	$T_n12 = 16.7 - 0.00519E - 0.246L$	90.3
<i>1961–1970</i>			
$T_x1 = 38.2 - 0.00673E - 0.529L$	98.0	$T_n1 = 15.9 - 0.00536E - 0.267L$	89.3
$T_x2 = 39.3 - 0.00691E - 0.495L$	97.9	$T_n2 = 15.9 - 0.00572E - 0.188L$	92.8
$T_x3 = 45.3 - 0.00686E - 0.524L$	97.3	$T_n3 = 21.8 - 0.00582E - 0.232L$	93.8
$T_x4 = 53.2 - 0.00713E - 0.589L$	97.7	$T_n4 = 30.0 - 0.00592E - 0.334L$	94.7
$T_x5 = 48.7 - 0.00766E - 0.281L$	97.8	$T_n5 = 35.1 - 0.00612E - 0.346L$	95.4
$T_x6 = 20.0 - 0.00828E + 0.703L$	96.6	$T_n6 = 31.6 - 0.00608E - 0.129L$	94.7
$T_x7 = -9.23 - 0.00727E + 1.48L$	90.3	$T_n7 = 17.1 - 0.00590E + 0.328L$	95.1
$T_x8 = -6.80 - 0.00701E + 1.37L$	88.3	$T_n8 = 17.0 - 0.00588E + 0.316L$	95.2
$T_x9 = 2.74 - 0.00751E + 1.06L$	95.4	$T_n9 = 27.1 - 0.00560E - 0.088L$	94.4
$T_x10 = 25.2 - 0.00765E + 0.288L$	98.0	$T_n10 = 22.8 - 0.00546E - 0.136L$	91.7
$T_x11 = 38.0 - 0.00706E - 0.281L$	98.3	$T_n11 = 20.7 - 0.00530E - 0.228L$	89.4
$T_x12 = 44.0 - 0.00654E - 0.632L$	96.9	$T_n12 = 14.2 - 0.00524E - 0.174L$	87.8

## 4.2 | Snow accumulation adjustments

The total ablation losses at a given ablation rate from a glacier zone depend on the ablation gradient and  $\Delta ELA$  (the difference between the mean elevation of a glacier zone and ELA). Assuming that the practical ablation above ELA is insignificant, the potential ablation losses from the selected glacier zones vary from 0 to 1,000 mm/year (Table 2). These ablation losses are added to the original estimates of the net accumulations to account for the ablation losses from the actual precipitation.

## 4.3 | Spatial distribution of unadjusted and adjusted precipitation

Continuous fields of precipitation generated through KED-based interpolation of the adjusted station observations and adjusted snow accumulations at monthly scale show how precipitation patterns and amounts are spatially distributed in the study area (Figure 3a–l). Monthly precipitation distributions largely confirm the bimodal weather system reflecting the wintertime precipitation associated with the westerlies and the impact of Indian summer monsoon in the study area. Overall climatology and distribution patterns of the adjusted precipitation (Figure 3m) match very well to the unadjusted case (Figure 3n) or estimates of Dahri et al. (2016). However, the adjustments revealed significant improvement in terms of quantitative and spatio-temporal distribution of precipitation in the study area (Figure 3o). An overall increase of 21.3% in average annual precipitation is realized at basin (study area) level, while at sub-basin scale it ranged from 6 to 77% (Table 3). Greatest improvements are achieved in the high-altitude areas of Astore, Shyok, Shigar, Hunza, Gilgit and Chitral sub-basin and during the winter months.

## 4.4 | River run-off adjustments

The net mass balance estimates of Käab et al. (2012) for the study area are translated into the amount of run-off generated at sub-basin scale. As a result of slightly negative mass balance estimates for all sub-basins, their contributions to river run-off are also negative and relatively small ranging from 0.4 to 6.1%. The adjustments in river-specific run-off depend on the net mass balance as well as glacier area and varied from  $-51.5$  mm in the Chenab sub-basin to  $-2.5$  mm in the Panjkora sub-basin (Table 4).

## 4.5 | Validation of precipitation estimates

The estimated precipitation distributions can be validated by evaluating the accuracy of the employed interpolation scheme and the output interpolated fields. For accuracy assessment of the interpolation scheme, the KED interpolation model produces both prediction as well as error/uncertainty surfaces, giving an indication or measure of how

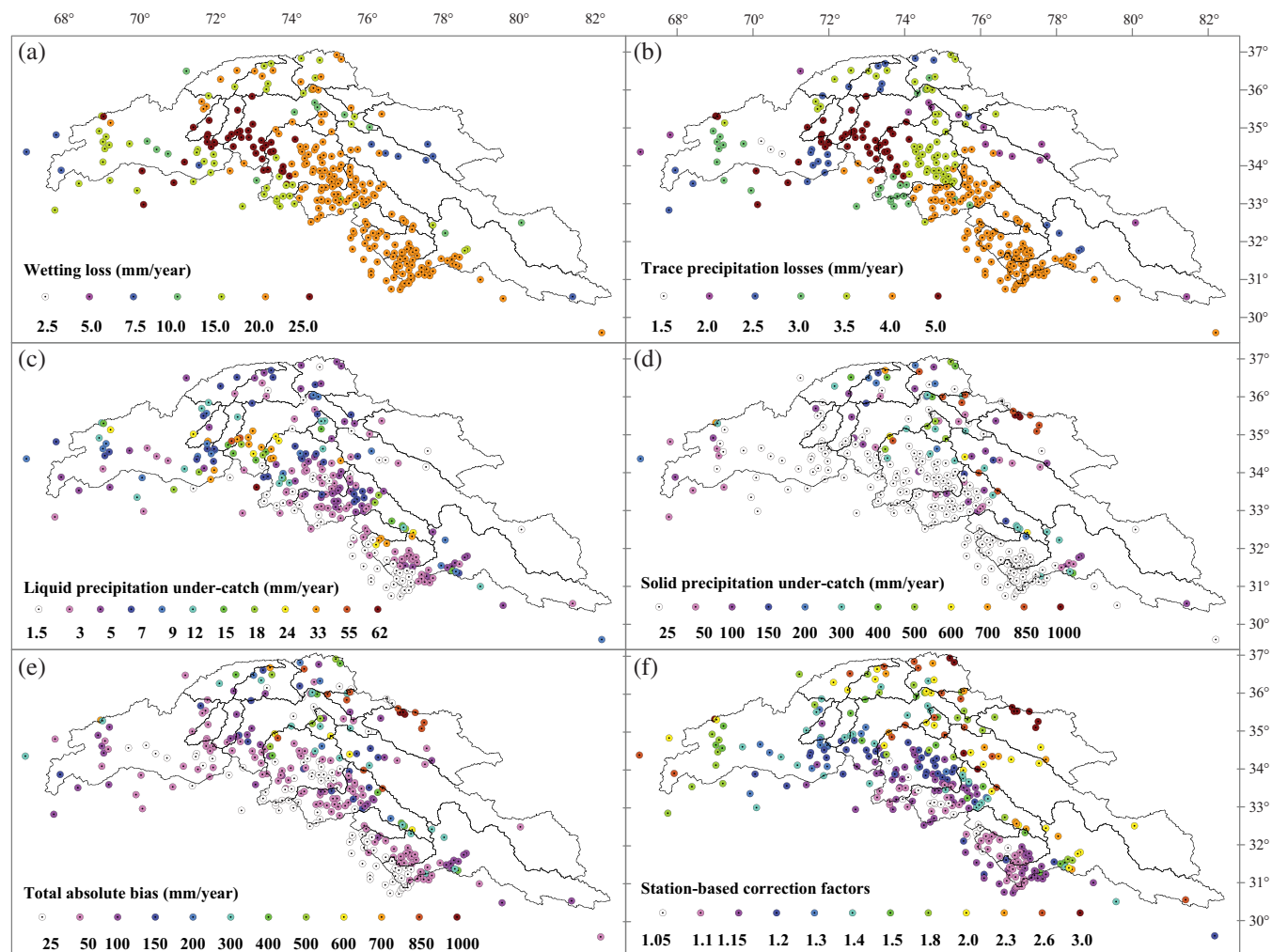


**FIGURE 2** Adjusted station observations for (a) wetting loss, (b) trace precipitation loss, (c) liquid precipitation under-catch, (d) solid precipitation under-catch, (e) total absolute bias between gauge-measured and error-adjusted annual precipitation, (f) station-based CFs for under-catch of gauge-measured precipitation. The different scales are to be noted [Colour figure can be viewed at [wileyonlinelibrary.com](http://wileyonlinelibrary.com)]

good the predictions are. The cross validation applied on the observed and predicted values from all the stations resulted in relative bias ( $B$ ) error scores of less than 1, suggesting a negligible underestimation of the predicted values for all months except August, which shows a slight overestimation (Table 5). Similarly, the relative mean root-transformed error ( $E$ ) scores of less than 1 for the months January–May suggest excellent results. While the remaining months of June–December experience  $E$  values of greater than 1, which depict typical errors slightly greater than the spatial variations. Almost similar trends are observed for the unadjusted case. In general, the cross-validation results depict excellent/good agreement between the observed and predicted values.

Another means of validation is the comparison of the estimated precipitation with the corresponding observed river flows (specific run-offs). Dahri et al. (2016) demonstrated that the previous estimates of precipitation distribution in the study area are not only highly contrasting but largely underestimating the actual precipitation. Likewise in

the Dahri et al. (2016) study, precipitation estimates derived from the unadjusted precipitation observations provided relatively better estimates than the previous studies. Yet, slightly lower precipitation than the measured specific runoff in 9 out of 17 sub-basins (Figure 4) is absolutely counterintuitive implying underestimated precipitation or an unaccounted source of water (e.g., glacier melt contribution). Long-term annual mean precipitation must always be greater than the corresponding specific runoff if a positive or neutral mass balance is prevalent in any river basin. In case of a negative mass balance, its contribution to river flows has to be subtracted from the actually observed river flows and the adjusted flows must be lower than the corresponding mean annual precipitation. Cross validation of adjusted precipitation estimates with the corresponding adjusted specific run-offs (Figure 4) revealed adjusted specific run-off well below the adjusted precipitation estimates for all the sub-basins except Swat, which reflects underestimated precipitation or a bigger contribution of a negative mass balance to river flows.

**TABLE 2** Adjusted net snow water equivalent at the major glacier accumulation zones. Lon. is longitude, Lat. is latitude, Ele. is elevation, ELA is equilibrium line altitude,  $\Delta$ ELA is the net elevation contributing to ablation and  $\Delta$ A is adjustment in the net accumulation

Glacier name	Lon. (dd)	Lat. (dd)	Ele. (m)	River basin	ELA (m)	$\Delta$ ELA (m)	$\Delta$ A (mm)	Net accum. (mm/year)	Adj. accum. (mm/year)
Approach	75.6331	36.0678	5,100	Shigar	5,050	0	0	1,880	1,880
Baltoro	76.5508	35.8778	5,500	Shigar	5,050	0	0	1,600	1,600
Batura	74.3833	36.6667	4,840	Hunza	5,000	160	800	1,034	1,834
Chogolungma	75.0000	36.0000	5,400	Hunza	5,000	150	750	1,070	1,820
Chong Kumdan	77.5448	35.2532	5,330	Shyok	5,500	170	850	484	1,334
Hispar Dome	75.5187	36.0109	5,450	Shigar	5,050	0	0	1,620	1,620
Hispar East	75.5064	35.8495	4,900	Shigar	5,050	150	750	1,070	1,820
Hispar West	75.5064	35.8495	4,830	Shigar	5,050	0	0	1,620	1,620
Hispar Pass	75.5215	36.0281	5,000	Shigar	5,050	50	250	1,420	1,670
Khurdopin	75.6197	36.1338	5,520	Shigar	5,050	0	0	2,240	2,240
Nanga Parbat	74.4444	35.1672	4,600	Astore	4,700	100	500	2,000	2,500
Nun Kun North	76.1014	34.1219	5,200	Shingo	5,250	50	250	900	1,150
Sentik	75.9500	33.9967	5,100	Shingo	5,250	150	750	620	1,370
Siachin A	77.0376	35.4707	5,300	Shyok	5,500	200	1,000	484	1,484
Siachin B	76.9915	35.5235	5,300	Shyok	5,500	200	1,000	526	1,526
Siachin C	76.9116	35.5187	5,320	Shyok	5,500	180	900	662	1,562
Siachin D	76.8592	35.6242	5,350	Shyok	5,500	150	750	855	1,605
South Terong	77.4516	35.1384	5,330	Shyok	5,500	170	850	484	1,334
Terong	77.3120	35.5177	5,350	Shyok	5,500	150	750	855	1,605
Urdok	76.7025	35.7669	5,400	Shigar	5,050	0	0	1,060	1,060
Whaleback	75.5915	36.0572	4,900	Shigar	5,050	150	750	1,790	2,540

## 5 | DISCUSSION

Precipitation is an integral component of the hydrological cycle and usually the most important input to water balance assessments and climate change studies. Hence, its accuracy is essential as errors in precipitation estimates may translate into major changes in the water budget of a particular region. However in many areas, precipitation measurements are still subject to significant errors and a large uncertainty (Kochendorfer et al., 2017a; Kochendorfer et al., 2018) often leading to a substantial underestimation of the actual precipitation. The situation is particularly serious in the high-altitude Indus basin where biased distribution and lack of the observed data further worsen the problem. As such the precipitation products derived from or validated by the observed data covering this region are prone to significant errors (Dahri et al., 2016; Reggiani & Rientjes, 2015). Scientists have used different approaches to overcome the observational data gaps. For example Adam et al. (2006) used a water balance approach to indirectly estimate precipitation. However, large uncertainties in the different water balance components limit wider application of this approach. Immerzeel et al. (2015) used mass balance estimates to inversely compute precipitation in the major snow/glacier zones and applied a linear lapse rate of precipitation increase with elevation up to 5,000 m using APHRODITE as the reference data set. Uncertainties in mass balance and

water balance components and assumption of linear precipitation increase with altitude are the major drawbacks of this method. Dahri et al. (2016) integrated station observations with the net snow accumulations estimated through mass balance studies and applied KED interpolation scheme to derive precipitation in ungauged areas. Measurement errors in station observations and negligence of snow/glacier ablations in the net snow accumulations are the key shortcomings of this approach.

The approach adopted in this study is based on catch adjustments of precipitation observations for systematic measurement errors, adjustment of net snow accumulations for the ablation losses and adjustment of river flows for the contribution of net GMB. Mean monthly precipitation climatologies are derived from the actual precipitation observations and actual net snow accumulations as well as from the adjusted precipitation observations and the adjusted net snow accumulations following Dahri et al. (2016).

The results presented in this study further support the wind-induced under-catch as the largest source of errors in gauge-measured precipitation observations. The catch corrections have increased the gauge-measured precipitation values ranging from 12 to 773 mm/year for various stations, while net snow accumulations at the glacier points increased up to 1,000 mm/year. A large part of precipitation in the high-altitude Indus basin falls as snow, which is more susceptible to under-catch even at moderate wind speeds. The

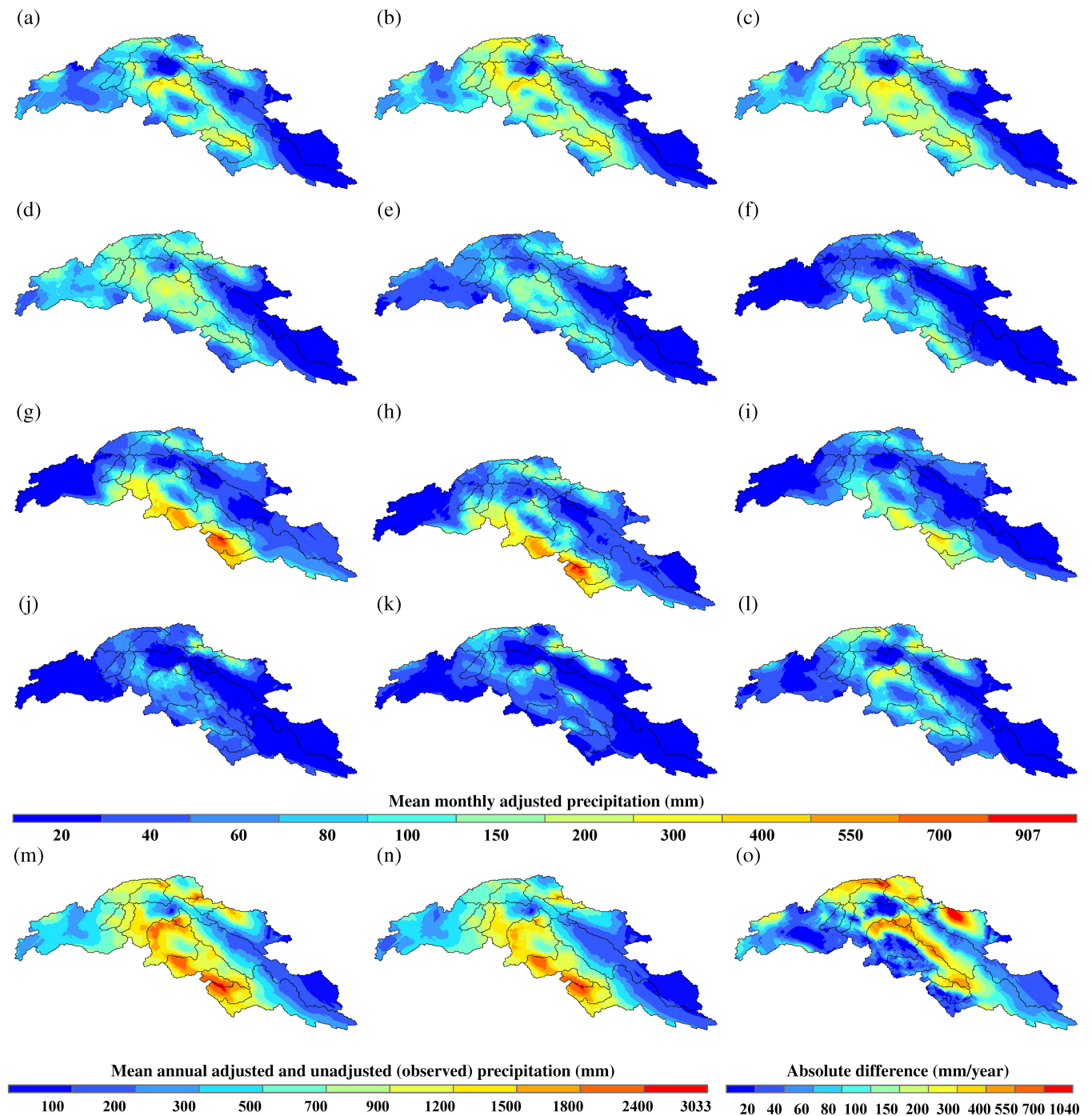


**FIGURE 3** Estimated precipitation distribution, (a–l) are mean monthly (January–December) error-adjusted precipitation, (m) is error adjusted annual precipitation, (n) is unadjusted annual precipitation based on actual observations and (o) is the absolute difference between adjusted and unadjusted annual precipitation distributions [Colour figure can be viewed at [wileyonlinelibrary.com](http://wileyonlinelibrary.com)]

largest corrections were found for wind-induced under-catch of solid precipitation, which is in line with the results of previous studies (e.g., Adam & Lettenmaier, 2003; Chen et al., 2015; Goodison et al., 1998; Kochendorfer et al., 2017a; Kochendorfer et al., 2018; Legates & Willmott, 1990; Michelson, 2004; Wolff et al., 2015; Yang, Kane, Zhang, Legates, & Goodison, 2005; Ye, Yang, Ding, Han, & Koike, 2004). However, liquid precipitation under-catch, wetting loss and trace precipitation loss are also important, particularly in low-altitude and relatively dry areas.

The large differences between the observed precipitation and the corresponding specific run-off observations (usually greater specific run-off than precipitation) in previous estimates are often attributed to the contribution of snow/glacier melt. Indeed the high-altitude Indus basin receives considerable snow/glacier melt contributions, which largely come from the melting of temporary/seasonal snow cover and may vary from year to year depending on the quantity and timing of winter snowfall and snowmelt during the subsequent summer. However, quantitative estimates of net GMB

**TABLE 3** Precipitation estimates at sub-basin scale.  $P_{\text{uadj}}$  is unadjusted precipitation derived through actual precipitation observations and net glacier accumulations,  $P_{\text{adj}}$  is adjusted precipitation derived through corrected precipitation observations and adjusted glacier accumulations and  $\Delta P$  is the difference between them

S. No.	River basin	$P_{\text{uadj}}$ (mm)	$P_{\text{adj}}$ (mm)	$\Delta P$ (mm)	Increase (%)
1	Gilgit at Gilgit	582.1	787.0	204.9	35.2
2	Hunza at Dainyor	601.2	879.9	278.7	46.4
3	Shigar at Shigar	829.8	1006.0	176.2	21.2
4	Shyok at Yugo	249.6	442.3	192.6	77.2
5	Indus at Kharhong	182.5	285.8	103.3	56.6
6	Astore at Doyian	917.8	1269.1	351.3	38.3
7	Indus at Tarbela dam	394.5	540.6	146.1	37.0
8	Chitral at Chitral	646.3	924.9	278.6	43.1
9	Panjhora at Zulum Br.	738.1	797.0	58.9	8.0
10	Swat at Chakdara	950.3	1050.5	100.2	10.5
11	Kabul at Warsak	391.7	488.3	96.6	24.7
12	Kabul at Nowshera	477.9	504.1	26.1	5.5
13	Jhelum at Mangla dam	1129.3	1271.0	141.7	12.5
14	Chenab at Marala	1106.4	1257.0	150.6	13.6
15	Ravi at Thein dam	1647.2	1812.1	164.9	10.0
16	Beas at Pong dam	1547.1	1635.7	88.6	5.7
17	Sutlej at Bhakra dam	358.5	444.5	86.1	24.0
	Whole basin	574.7	697.3	122.6	21.3

contributions to river flows are largely lacking. Therefore, the accuracy of the estimated net GMB contributions to the river flows is mainly depending on the uncertainties in glacier area and the ablation rates of mass balance. Our methodology of adjusting river flows for the net mass balance contributions is straight forwards and the adjustments are slightly less than what is modelled by Lutz et al. (2016). For example, we estimated net GMB contribution of  $-17.3$  mm/year for the Indus at Besham Qila against  $-25.0$  mm/year modelled by Lutz et al. (2016). The difference might be due to the use of different approaches and different glacier inventories having different glacier areas. Lutz et al. (2016) pointed out a 23% difference in the glacier areas from three different inventories implying considerable differences in the water balance components.

The precipitation distribution derived through actual station observations combined with the actual net glacier accumulations is almost similar to that derived by Dahri et al. (2016) except for the addition of a few sub-basins and the use of additional and updated observed data. The catch corrections and snow accumulation adjustments

significantly increased the total gauge-measured as well as basin-scale precipitation (Figures 2–3o and 4 and Table 3). The overall distribution patterns of precipitation remained largely the same as identified by Dahri et al. (2016), but substantial increases in the magnitude of precipitation amounts are realized. One of the advantages of the KED interpolation method is that it estimates an interpolated surface from a randomly varied small set of measured points and recalculates estimated values for these measured points to validate the estimates and determine the extent of errors. When compared with the corrected precipitation derived by Immerzeel et al. (2015), our estimates show significantly smaller root-mean-square error and a stronger correlation with the error-adjusted station observations (Figure 5). The corrected precipitation estimates by Immerzeel et al. (2015) show considerable differences with significantly lower values at the majority of station locations including the points at the major glaciers, where actual measurements of net snow accumulations were taken. At the basin scale their estimates are relatively better but seem to be on the higher side in about half of the sub-basins. This discrepancy between station-based point observations and basin-scale precipitation estimates by Immerzeel et al. (2015) may be attributed to the higher and linear lapse rates of precipitation increase applied to compute the precipitation fields. Also, they did not validate their estimates with the observed precipitation of the individual stations. Instead, they used the Turc-Budyko representation to show the physical realism of their estimates and attributed some of the estimates that fall on the right side (inside) of the theoretical Budyko curve to the possible contribution of the negative mass balance to river flows and uncertainties in the potential evapotranspiration ( $ET_p$ ) data set.

In this study, we used accurate run-off observations (specific run-offs), which are further improved by adjusting for the net GMB contributions, and improved  $ET_p$  estimates from JRA55 reanalysis data set (Figure 6) to evaluate the physical realism of our estimated precipitation compared to the precipitation estimates from Immerzeel et al. (2015). Over one third of the points representing estimated precipitation by Immerzeel et al. (2015) in various sub-basins (e.g., Gilgit, Chitral, Panjkora, Kabul at Warsak and Nowshera, and Sutlej) lay inside the theoretical Budyko curve indicating higher values than the theoretically expected. However, the estimates of unadjusted precipitation in our study, which are almost similar to the estimates of Dahri et al. (2016), show 10 out of 17 sub-basins above the line of moisture limit indicating underestimated precipitation in these sub-basins. The adjusted precipitation derived in our study shows relatively better fits in the Turc-Budyko representation except for the Swat sub-basin. The greater specific run-off than precipitation in the Swat basin may be attributed to yet an underestimated precipitation and/or greater negative mass balance than what is presently assumed.

TABLE 4 Contribution of net GMB to river flows and adjusted specific run-off

S. No.	River basin name	Glacier area (km <sup>2</sup> )	Net GMB (m/year)	Contribution of net GMB to river flows (mm/year)	Observed sp. run-off (mm/year)	Adjusted sp. run-off (mm/year)
1	Gilgit at Gilgit	1212.5	-0.350	-33.3	758.0	724.7
2	Hunza at Dainyor	4268.7	-0.113	-35.4	680.1	644.7
3	Shigar at Shigar	2974.1	-0.090	-38.1	924.9	886.8
4	Shyok at Yugo	7400.4	-0.060	-13.0	365.5	352.5
5	Indus at Kharhong	2164.7	-0.326	-9.9	201.3	191.4
6	Astore at Doyian	257.7	-0.540	-35.1	1136.7	1101.6
7	Indus at Tarbela dam	19355.3	-0.150	-16.7	421.2	404.6
8	Chitral at Chitral	1736.3	-0.320	-44.8	737.2	692.4
9	Panjhora at Zulum Br.	41.0	-0.350	-2.5	616.5	614.0
10	Swat at Chakdara	202.6	-0.400	-14.1	1186.3	1172.2
11	Kabul at Warsak	1851.5	-0.340	-8.9	154.8	145.9
12	Kabul at Nowshera	2095.0	-0.340	-7.9	305.6	297.7
13	Jhelum at Mangla dam	262.7	-0.550	-4.3	792.8	788.5
14	Chenab at Marala	2667.4	-0.560	-51.5	1026.4	975.0
15	Ravi at Thein dam	166.9	-0.386	-10.5	1391.0	1380.5
16	Beas at Pong dam	511.0	-0.213	-8.7	986.5	977.8
17	Sutlej at Bhakra dam	1411.9	-0.359	-9.3	264.2	254.9

TABLE 5 Relative bias (*B*) and relative mean root-transformed error (*E*) calculated over all observation points

	Jan	Feb	Mar	Apr	May	Jun	Jul	Aug	Sep	Oct	Nov	Dec	Ann
B	0.924	0.964	0.955	0.963	0.953	0.936	0.973	1.002	0.997	0.877	0.916	0.908	0.957
E	0.957	0.941	0.912	0.918	0.909	1.338	1.955	9.541	3.306	1.762	3.372	1.055	2.801

The run-off ratio ( $Q/P$ ) determines the amount of precipitation converted into overland flow or surface run-off. It is mainly controlled by largely stable natural factors including climate, soil and topography and to some extent by the human alterations to landscapes. Relatively higher run-off ratios are produced for areas with shallow or clay soils, steeper slopes and devoid of vegetation cover. Snow-covered areas hold winter precipitation as snow/ice and produce higher run-off ratios during the subsequent snow melting periods. Over 50% of the study area possesses slopes steeper than 40% and about 81% of the surface soil type is leptosol (47.4%), cambisol (22.5%) and rock outcrop (11.1%). Dominant land cover types are closed to open herbaceous vegetation (34.6%), bare rocky areas (25.3%) and permanent snow and glaciers (13.4%) (Figure S6). All these topographical properties infer the high-altitude Indus basin as a typical case of an area that accelerates rapid run-off generation. Therefore, relatively high rates of run-off ratios are to be expected. Table S4 and Figure 6 show the improved run-off ratios ( $Q/P$ ) and aridity indices ( $P/ET_p$ ) if compared to the data sets of Dahri et al. (2016) and Immerzeel et al. (2015).

Although the error-adjusted precipitation derived in this study seems to be more consistent, yet there are a few uncertainties that need to be understood and taken care of in future investigations. The major uncertainties associated with the results of our study may arise from four possible

sources: (a) uncertainties in regression models due to their imprecision and uncertainties in the input data, (b) uncertainties arising from the estimated temperature and wind speed for many observatories, (c) uncertainty in the gauge type of the basin's gauge network and (d) uncertainties in spatial interpolation of the point observations to derive gridded fields of precipitation. The error estimation of the regression models employed in this study are tested at different locations and the relationships with the best fit are also applicable for similar situations in other areas. Nevertheless, regression models are in essence approximations of reality and some degree of uncertainty will always remain in the results. Relatively more accurate adjustments of precipitation under-catch for any precipitation event can be made by using the corresponding data of temperature and wind speed. However, hourly or daily data of these parameters are not available for many observatories in the study area. Also, there are many stations for which such data are not available at all. For locations without these data, temperature may be derived from the lapse rates of the available observations and wind speed from JRA55 data set. However as shown, the use of these data may add to the uncertainties in the catch corrections. The meteorological data collecting agencies in the Indus basin generally indicate to follow the WMO standards but we found inconsistencies in the use of precipitation measurement instruments and techniques. As the correction coefficients to account for

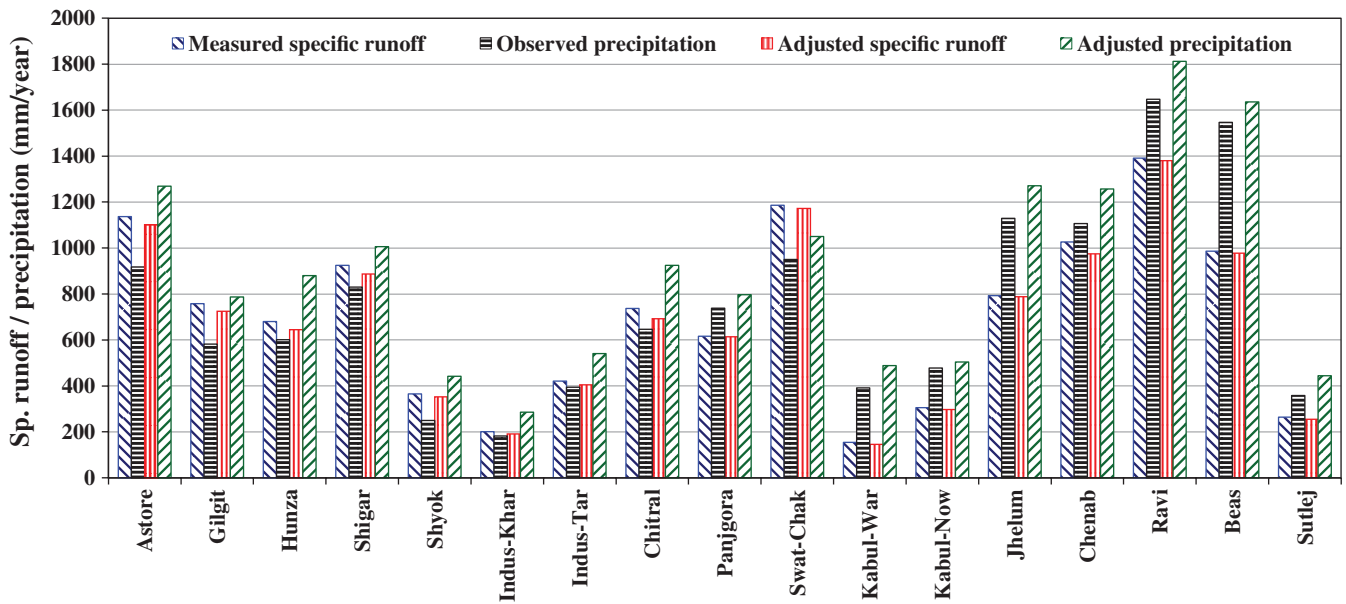


FIGURE 4 Annual measured and adjusted specific run-off and annual observed and adjusted precipitation at sub-basin scale [Colour figure can be viewed at wileyonlinelibrary.com]

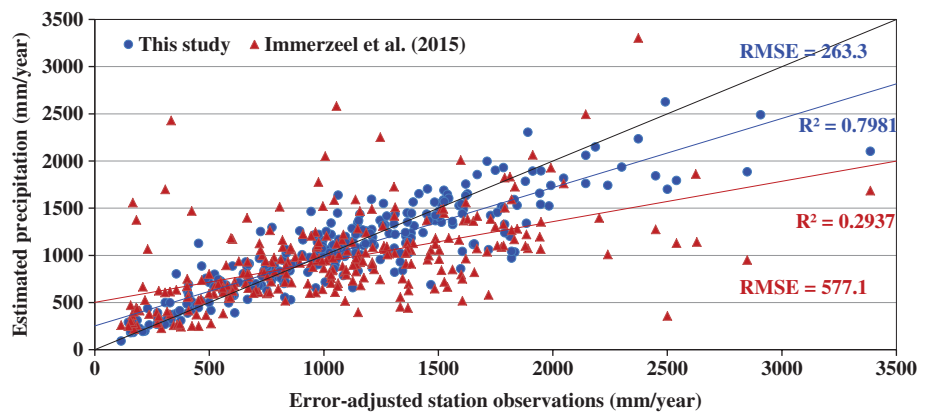


FIGURE 5 Comparison of error adjusted station observations with the corresponding estimated values under this study and by Immerzeel et al. (2015) [Colour figure can be viewed at wileyonlinelibrary.com]

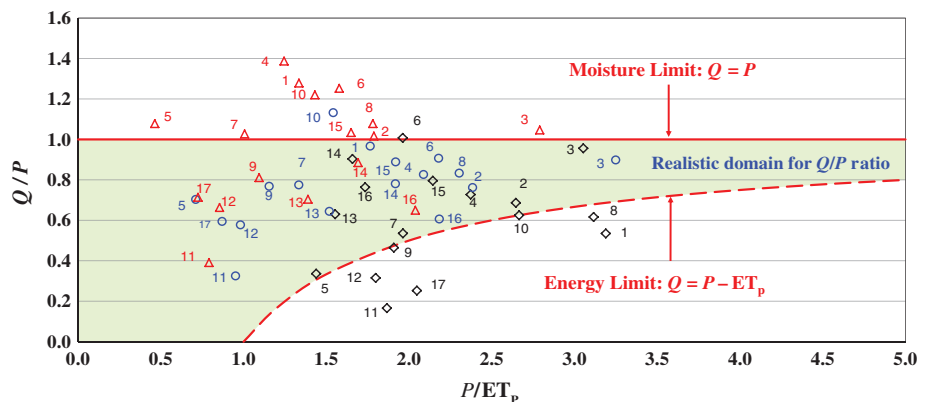


FIGURE 6 Turc-Budyko representation of run-off ratio ( $Q/P$ ) and aridity index ( $P/ET_p$ ). The red triangles display estimates of unadjusted case or Dahri et al. (2016), black diamonds show estimates of Immerzeel et al. (2015) and blue circles indicate adjusted estimates under this study. The numbers refer to the sub-basins as given in Table 4 [Colour figure can be viewed at wileyonlinelibrary.com]

wind-induced under-catch of precipitation depend on the type and orifice area of the precipitation gauge, incorrect gauge configuration information has consequences for the catch corrections. Although we tried our best to obtain the maximum possible information regarding the type and specs of precipitation gauges, we cannot exclude the chances of different precipitation gauges than the actual ones in some cases. However, we also think that the possibility of slight

differences in gauge type will only have a small impact on the final results. The uncertainties resulting from spatial interpolation techniques described by Dahri et al. (2016) are equally applicable for this study as we followed their interpolation approach. Importantly, the cross-validation results infer high accuracy of the corrections and indicate excellent agreement between the adjusted precipitation and adjusted specific run-off at sub-basin scale.

## 6 | CONCLUSIONS

Reliable estimates of precipitation climatologies and amounts in the high-altitude Indus basin are seriously constrained by the quality and number of observed data (e.g., scarcity of in situ observations, measurement errors and space–time breaks). This study attempted to address these core issues by improved estimates of the precipitation measurement errors and integrating precipitation data from multiple sources with the net snow accumulations at major glacier zones. The study employed WMO recommended standard methods to adjust systematic errors in precipitation measurements. Simple methods to adjust net snow accumulation for the ablation losses and adjustment of river flows for the net mass balance contributions are introduced. Mean monthly adjusted and unadjusted precipitation observations and net snow accumulations are spatially interpolated using the KED interpolation scheme. Analysis of temperature variations with elevation and latitude revealed significantly different gradients for each month and substantial differences among the gradients at different locations for maximum and minimum temperatures. Hence, the use of a universal annual gradient or a time-independent gradient of mean temperature to estimate maximum and minimum temperatures or vice versa is a major source of uncertainty for the high-altitude Indus basin.

The applied error-adjustments significantly increased the gauge-measured precipitation, which is in line with previous studies. The total bias between gauge-measured and error-adjusted precipitation ranged from 12 to 773 mm/year (2–182%) for various individual stations. The highest increments are computed for wind-induced under-catch of solid precipitation, particularly in higher-altitude areas and during winter months. The range of liquid precipitation under-catch is much smaller concentrating mainly in the low-altitude areas during summer monsoon. Similarly, notable increases varying from 0 to 1,000 mm/year (0–200%) are estimated for net snow accumulations. Precipitation increase at the basin (study area) scale is 21.3%, while at sub-basin scale it ranged from 6 to 77% with greater increments at higher-altitude areas and during winter months. Contrary to the general understanding, the contribution of net GMB to river flows is only marginal ranging from 0.5 to 6.1% of the observed flows. The highest contributions are revealed for the Chenab, Chitral, Shigar, Hunza, Astore and Gilgit basins.

The cross-validation results (Figure 4) and the Turc-Budyko representation of the run-off ratios and aridity indices at sub-basin scale (Figure 5) show that the adjusted precipitation amounts and distribution patterns derived in this study are more accurate than the unadjusted data and previous estimates. The catch corrections provided new insights in the magnitude and distribution patterns of precipitation implying potential hydrological implications for

water resources assessment, planning and management. The actual precipitation is considerably greater than what has been previously thought. These increases are mainly realized in the higher-altitude areas of Chitral, Gilgit, Hunza, Shigar, Shyok and Astore basins. The study recognizes that the data quality-driven underestimated precipitation may be the major source of uncertainty in the water balance estimates in the high-altitude Indus basin. The improved climatologies of mean monthly precipitation developed in this study can be used for basin or sub-basin-scale water balance studies and bias correction of gridded precipitation products, thereby paving the way for the development of an accurate, consistent and high-resolution gridded precipitation product for this highly under-explored region of the Indus basin.

Although our estimates of precipitation distribution can easily be regarded as much better than currently available estimates, the uncertainties elaborated at the end of the previous section recognize the need for further improvement. Further improvements can be achieved by calibration of the already installed precipitation gauges with the WMO recommended reference gauges and development of site and gauge-specific error adjustment models, use of observed data with better spatio-temporal coverage, use of daily or even sub-daily time steps, use of corresponding observed wind speed and temperature data sets, selection of any better spatial interpolation technique, accuracy assessment and precise determination of other components of the water balance to validate precipitation, and a better integration of precipitation data with mass balance data.

## ACKNOWLEDGEMENTS

This research work was supported by the Dutch Ministry of Foreign Affairs through The Netherlands Fellowship Program (NFP) and carried out by the Himalayan Adaptation, Water and Resilience (HI-AWARE) consortium under the Collaborative Adaptation Research Initiative in Africa and Asia (CARIAS) with financial support from the Department for International Development, UK Government and the International Development Research Centre, Ottawa, Canada. A part of this work was undertaken at the International Institute for Applied System Analysis (IIASA), Laxenburg, Austria under the Young Scientist Summer Program (YSSP) 2016 with financial support provided by the Netherlands Organization for Scientific Research. The views expressed in this work do not necessarily represent those of the supporting organizations. The authors express their deepest gratitude to WAPDA and PMD for sharing the hydro-meteorological data of the study region. We also acknowledge Arthur F. Lutz and Jennifer C. Adam for providing their precipitation data sets for comparison and further analysis in this study.



## Conflict of interests

The authors declare no potential conflict of interests.

## ORCID

Zakir Hussain Dahri  <http://orcid.org/0000-0002-0922-951X>

## REFERENCES

- Adam, J. C., Clark, E. A., Lettenmaier, D. P., & Wood, E. F. (2006). Correction of global precipitation products for orographic effects. *Journal of Climate*, 19(1), 15–38.
- Adam, J. C., & Lettenmaier, D. P. (2003). Adjustment of global gridded precipitation for systematic bias. *Journal of Geophysical Research*, 108, 4257. <https://doi.org/10.1029/2002JD002499>
- Adeloye, A. J., Remesan, R., & Soundharajan, B. S. (2016). Effect of hedging-integrated rule curves on the performance of the Pong Reservoir (India) during scenario-neutral climate change perturbations. *Water Resources Management*, 30, 445–470. <https://doi.org/10.1007/s11269-015-1171-z>
- Akhtar, M., Ahmad, N., & Booi, M. J. (2008). The impact of climate changes on the water resources of Hindukush–Karakorum–Himalaya region under different glacier coverage scenarios. *Journal of Hydrology*, 355, 148–163. <https://doi.org/10.1016/j.jhydrol.2008.03.015>
- Arendt, A., Bliss, A., Bolch, T., Cogley, J. G., Gardner, A. S., Hagen, J.-O., ... Zhelytshina, N. (2015). *Randolph glacier inventory—A dataset of global glacier outlines: Version 5.0* (GLIMS Technical Report).
- Arora, M., Singh, P., Goel, N. K., & Singh, R. D. (2006). Spatial distribution and seasonal variability of rainfall in a mountainous basin in the Himalayan region. *Water Resources Management*, 20, 489–508. <https://doi.org/10.1007/s11269-006-8773-4>
- Asian Development Bank. (2010). *INDIA: Integrated water resources management scoping study for Sutlej River basin, Himachal Pradesh: Improving capacity for climate change adaptation*, Technical assistance consultant's report, part 2—Main report (Project No. 43169).
- Batura Investigations Group. (1979). The Batura glacier in the Karakoram mountains and its variations. *Scientia Sinica*, 22, 958–974.
- Bhutiyani, M. R. (1999). Mass balance studies on Siachen glacier in the Nubra valley, Karakoram Himalaya, India. *Journal of Glaciology*, 45(149), 112–118.
- Biemans, H., Hutjes, R. W. A., Kabat, P., Strengers, B. J., Gerten, D., & Rost, S. (2009). Effects of precipitation uncertainty on discharge calculations for main river basins. *Journal of Hydrometeorology*, 10, 1011–1025.
- Bindoff, N. L., Stott, P. A., AchutaRao, K. M., Allen, M. R., Gillett, N., Gutzler, D., ... Zhang, X. (2013, 2013). Detection and attribution of climate change. In T. F. Stocker, D. Qin, G.-K. Plattner, M. Tignor, S. K. Allen, J. Boschung, et al. (Eds.), *Climate change 2013: The physical science basis. Contribution of working group I to the fifth assessment report of the Intergovernmental Panel on Climate Change* (pp. 867–952). Cambridge, England; New York, NY: Cambridge University Press.
- Bocchiola, D., Diolaiuti, G. A., Soncini, A., Mihalcea, C., D'Agata, C., Mayer, C., ... Smiraglia, C. (2011). Prediction of future hydrological regimes in poorly gauged high altitude basins: The case study of the upper Indus, Pakistan. *Hydrology and Earth System Sciences*, 15, 2059–2075.
- Bookhagen, B., & Burbank, D. W. (2010). Toward a complete Himalayan hydrological budget: Spatiotemporal distribution of snowmelt and rainfall and their impact on river discharge. *Journal of Geophysical Research: Earth Surface*, 115(3), 2003–2012.
- Budyko, M. I. (1974). *Climate and life* (508 pp.). Orlando, FL: Academic Press.
- Bureau of Indian Standards (BIS). (1992a). IS 5225. 1992. Meteorology - Rain-gauge, non-recording [PGD 21: Meteorological Instruments]. New Delhi, India: Author.
- Bureau of Indian Standards (BIS). (1992b). IS 5235. 1992. Meteorology - Rain-gauge, recording [PGD 21: Meteorological Instruments]. New Delhi, India: Author.
- Businger, J. A., & Yaglom, A. M. (1971). Introduction to Obukhov's paper "Turbulence in an atmosphere with a non-uniform temperature". *Boundary-Layer Meteorology*, 2, 3–6.
- Chen, R., Liu, J., Kang, E., Yang, Y., Han, C., Liu, Z., ... Zhu, P. (2015). Precipitation measurement intercomparison in the Qilian Mountains, north-eastern Tibetan Plateau. *The Cryosphere*, 9, 1995–2008.
- Cruz, R. V., Harasawa, H., Lal, M., Wu, S., Anokhin, Y., Punsalma, B., ... Ninh, N. H. (2007). Asia. In M. L. Parry, O. F. Canziani, J. P. Palutikof, P. J. van der Linden, & C. E. Hanson (Eds.), *Climate change 2007: Impacts, adaptation and vulnerability, contribution of working group II to the fourth assessment report of the Intergovernmental Panel on Climate Change* (pp. 469–506). Cambridge, England: Cambridge University Press.
- Cuffey, K. M., & Paterson, W. S. B. (2010). *The physics of glaciers* (4th ed., 693 pp.). Oxford, England: Butterworth-Heinemann, Elsevier.
- Central Water Commission and National Remote Sensing Centre. (2014). *Indus basin, version 2.0*. Bhopal, India: Author.
- Dahri, Z. H., Ludwig, F., Moors, E., Ahmad, B., Khan, A., & Kabat, P. (2016). An appraisal of precipitation distribution in the high-altitude catchments of the Indus basin. *Science of the Total Environment*, 548–549, 289–306.
- Decheng, M. (1978). *The map of snow mountains in China, K2 (Mount Quogori), Lanzhou*. Lanzhou, China: Lanzhou Institute of Glaciology and Cryology, Chinese Academy of Sciences.
- Diggle, P. J., & Ribeiro, P. J. (2007). *Model-based geostatistics Springer series in statistics* (). New York, NY: Springer.
- Eberhardt, E., Dickore, W. B., & Mieke, G. (2007). Vegetation map of the Batura valley (north Pakistan). *Erkundung*, 61, 93–112.
- Goodison, B. E., Louie, P. Y. T., & Yang, D. (1998). *WMO solid precipitation measurement intercomparison, Instruments and observing methods* (Final Report No. 67, WMO/TD-No. 872). Geneva, Switzerland: World Meteorological Organization.
- Harding, R. J., Blyth, E. M., Tuinenburg, O. A., & Wiltshire, A. (2013, 2013). Land atmosphere feedbacks and their role in the water resources of the Ganges basin. *Science of the Total Environment*, 468–469, S85–S92. <https://doi.org/10.1016/j.scitotenv.2013.03.016>
- Hewitt, K. (2005). The Karakoram anomaly? Glacier expansion and the "elevation effect," Karakoram Himalaya. *Mountain Research and Development*, 25, 332–340. [https://doi.org/10.1659/0276-4741\(2005\)025\[0332:TKAGEA\]2.0.CO;2](https://doi.org/10.1659/0276-4741(2005)025[0332:TKAGEA]2.0.CO;2)
- Hewitt, K. (2011). Glacier change, concentration, and elevation effects in the Karakoram Himalaya, upper Indus basin. *Mountain Research and Development*, 31(3), 188–200. <https://doi.org/10.1659/mrd-journal-d-11-00020.1>
- Hewitt, K., Wake, C., Young, G. J., & David, C. (1989). Hydrological investigations at Biafo glacier, Karakoram Himalaya, Pakistan: An important source of water for the Indus River. *Annals of Glaciology*, 13, 103–108.
- Immerzeel WW, Droogers P, de Jong SM, Bierkens M. F. P. 2009. Large-scale monitoring of snow cover and runoff simulation in Himalayan river basins using remote sensing. *Remote Sensing of Environment* 113, 40–49.
- Immerzeel, W. W., Droogers, P., de Jong, S. M., Bierkens, M. F. P. (2010). Satellite derived snow and runoff dynamics in the upper Indus river basin. *Grazer Schriften der Geographie und Raumforschung Band*, 45/2010, 303–312.
- Immerzeel, W. W., Pellicciotti, F., & Shrestha, A. B. (2012). Glaciers as a proxy to quantify the spatial distribution of precipitation in the Hunza basin. *Mountain Research and Development*, 32(1), 30–38. <https://doi.org/10.1659/MRD-JOURNAL-D-11-00097.1>
- Immerzeel, W. W., Van Beek, L. P. H., Konz, M., Shrestha, A. B., & Bierkens, M. F. P. (2012). Hydrological response to climate change in a glacierized catchment in the Himalayas. *Climatic Change*, 110, 721–736. <https://doi.org/10.1007/s10584-011-0143-4>
- Immerzeel, W. W., Wanders, N., Lutz, A. F., Shea, J. M., & Bierkens, M. F. P. (2015). Reconciling high altitude precipitation in the upper Indus basin with glacier mass balances and runoff. *Hydrology and Earth System Sciences*, 19, 4673–4687. <https://doi.org/10.5194/hessd-12-4755-2015>
- Kääb, A., Berthier, E., Christopher, N., Gardelle, J., & Arnaud, Y. (2012). Contrasting patterns of early twenty-first-century glacier mass change in the Himalayas. *Nature*, 488(7412), 495–498.
- Khan, A., Naz, B. S., & Bowling, L. C. (2015). Separating snow, clean and debris covered ice in the upper Indus basin, Hindukush–Karakoram–Himalayas, using Landsat images between 1998 and 2002. *Journal of Hydrology*, 521(2015), 46–64.
- Kick, W. (1980). Material for a glacier inventory of the Indus drainage basin—The Nanga Parbat massif, World Glacier Inventory. In *Proceedings of the Riederalp workshop* (Vol. 126, pp. 105–109). IAHS-AISH Publication.

- Kobayashi, S., Ota, Y., Harada, Y., Ebata, A., Moriya, M., Onoda, H., ... Takahashi, K. (2015). The JRA-55 reanalysis: General specifications and basic characteristics. *Journal of the Meteorological Society of Japan*, 93(1), 5–48. <https://doi.org/10.2151/jmsj.2015-001>
- Kochendorfer, J., Nitu, R., Wolff, M., Mekis, E., Rasmussen, R., Baker, B., ... Poikonen, A. (2017a). Analysis of single-Alter-shielded and unshielded measurements of mixed and solid precipitation from WMO-SPICE. *Hydrology and Earth System Sciences*, 21, 3525–3542. <https://doi.org/10.5194/hess-21-3525-2017>
- Kochendorfer, J., Nitu, R., Wolff, M., Mekis, E., Rasmussen, R., Baker, B., ... Jachcik, A. (2018). Testing and development of transfer functions for weighing precipitation gauges in WMO-SPICE. *Hydrology and Earth System Sciences*, 22, 1437–1452. <https://doi.org/10.5194/hess-22-1437-2018>
- Kochendorfer, J., Rasmussen, R., Wolff, M., Baker, B., Hall, M. E., Landolt, S., ... Leeper, R. (2017b). The quantification and correction of wind-induced precipitation measurement errors. *Hydrology and Earth System Sciences*, 21, 1973–1989. <https://doi.org/10.5194/hess-21-1973-2017>
- Legates, D. R. (1987). A climatology of global precipitation. *Publications in Climatology*, 40(1), 85.
- Legates, D. R., & Willmott, C. J. (1990). Mean seasonal and spatial variability in gauge-corrected global precipitation. *International Journal of Climatology*, 10, 111–127.
- Lutz, A. F., Immerzeel, W. W., Gobiet, A., Pellicciotti, F., & Bierkens, M. F. P. (2013). Comparison of climate change signals in CMIP3 and CMIP5 multi-model ensembles and implications for central Asian glaciers. *Hydrology and Earth System Sciences*, 17(9), 3661–3677. <https://doi.org/10.5194/hess-17-3661-2013>
- Lutz, A. F., Immerzeel, W. W., & Kraaijenbrink, P. D. A. (2014). *Gridded meteorological datasets and hydrological modelling in the upper Indus basin* (Final Report). Wageningen, The Netherlands: International Centre for Integrated Mountain Development (ICIMOD), FutureWater.
- Lutz, A. F., Immerzeel, W. W., Kraaijenbrink, P. D. A., Shrestha, A. B., & Bierkens, M. F. P. (2016). Climate change impacts on the upper Indus hydrology: Sources, shifts and extremes. *PLoS One*, 11(11), e0165630. <https://doi.org/10.1371/journal.pone.0165630>
- Lutz, A. F., Immerzeel, W. W., Shrestha, A. B., & Bierkens, M. F. P. (2014). Consistent increase in high Asia's runoff due to increasing glacier melt and precipitation. *Nature Climate Change*, 4, 587–592. <https://doi.org/10.1038/nclimate2237>
- Mayer, C., Lambrecht, A., Belò, M., Smiraglia, C., & Diolaiuti, G. (2006). Glaciological characteristics of the ablation zone of Baltoro glacier, Karakoram, Pakistan. *Annals of Glaciology*, 43(1), 123–131. <https://doi.org/10.3189/172756406781812087>
- Mayer, C., Lambrecht, A., Oerter, H., Schwikowski, M., Vuillemoz, E., Frank, N., & Diolaiuti, G. (2014). Accumulation studies at a high elevation glacier site in central Karakoram. *Advances in Meteorology*, 2014, 215162. <https://doi.org/10.1155/2014/215162>
- Mayewski, P. A., Lyons, W. B., & Ahmad, N. (1983). Chemical composition of a high altitude fresh snowfall in the Ladakh Himalayas. *Geophysical Research Letters*, 10(1), 105–108. <https://doi.org/10.1029/GL010i001p00105>
- Mayewski, P. A., Lyons, W. B., Ahmad, N., Smith, G., & Pourchet, M. (1984). Interpretation of the chemical and physical time series retrieved from Sentik glacier, Ladakh Himalaya, India. *Journal of Glaciology*, 30(104), 66–76.
- Michelson, D. B. (2004). Systematic correction of precipitation gauge observations using analyzed meteorological variables. *Journal of Hydrology*, 290(2004), 161–177.
- Miehe, S., Cramer, T., Jacobsen, J. P., & Winiger, M. (1996). Humidity conditions in the western Karakoram as indicated by climatic data and corresponding distribution patterns of the montane and alpine vegetation. *Erdkund.*, 50, 190–204.
- Miehe, S., Winiger, M., Bohner, J., & Yili, Z. (2001). The climate diagram map of high Asia. *Erdkund.*, 55, 94–97.
- Mishra, V. (2015). Climatic uncertainty in Himalayan water towers. *Journal of Geophysical Research: Atmospheres*, 120, 2689–2705. <https://doi.org/10.1002/2014JD022650>
- Mukhopadhyay, B. (2012). Detection of dual effects of degradation of perennial snow and ice covers on the hydrologic regime of a Himalayan River basin by stream water availability modeling. *Journal of Hydrology*, 412–413, 14–33. <https://doi.org/10.1016/j.jhydrol.2011.06.005>
- Nitu, R., & Wong, K. (2010). *CIMO survey on national summaries of methods and instruments for solid precipitation measurement at automatic weather stations*, Instruments and observing methods (Report No. 102, WMO/TD No. 1544). Geneva, Switzerland: World Meteorological Organization.
- Obukhov, A. M. (1971). Turbulence in an atmosphere with a non-uniform temperature. *Boundary-Layer Meteorology*, 2, 7–29.
- Palazzi, E., von Hardenberg, J., & Provenzale, A. (2013). Precipitation in the Hindu-Kush Karakoram Himalaya: Observations and future scenarios. *Journal of Geophysical Research: Atmospheres*, 118(1), 85–100. <https://doi.org/10.1029/2012JD018697>
- Pellicciotti, F., Buergi, C., Immerzeel, W. W., Konz, M., & Shrestha, A. B. (2012). Challenges and uncertainties in hydrological modeling of remote Hindu Kush–Karakoram–Himalayan (HKH) basins: Suggestions for calibration strategies. *Mountain Research and Development*, 32(1), 39–50. <https://doi.org/10.1659/MRD-JOURNAL-D-11-00092.1>
- Qazi, N. A. (1973). *Water resources development in Suru basin (Ladakh)* (Vol. 51, p. 1973). Srinagar, India: Vacant Press.
- Ragetti, S., & Pellicciotti, F. (2012). Calibration of a physically based spatially distributed hydrological model in a glacierized basin: On the use of knowledge from glaciometeorological processes to constrain model parameters. *Water Resources Research*, 48, 1–20. <https://doi.org/10.1029/2011WR010559>
- Reggiani, P., & Rientjes, T. H. M. (2015). A reflection on the long-term water balance of the upper Indus basin. *Hydrology Research*, 46, 446–462. <https://doi.org/10.2166/nh.2014.060>
- Schabenberger, O., & Gotway, C. A. (2005). *Statistical methods for spatial data analysis*. Boca Raton, FL: Chapman and Hall/CRC.
- Schaeffli, B., Hingray, B., Niggli, M., & Musy, A. (2005). A conceptual glacio-hydrological model for high mountainous catchments. *Hydrology and Earth System Sciences*, 9(1/2), 95–109. <https://doi.org/10.5194/hess-9-95-2005>
- Sevruk, B. (1982). *Methods of correction for systematic error in point precipitation measurement for operational use* (Operational Hydrology Report 589, 91 pp.). Geneva, Switzerland: World Meteorological Organization.
- Sevruk, B., & Hamon, W. R. (1984). *International comparison of national precipitation gauges with a reference pit gauge*, Instruments and observing methods (Report No. 17, 135 pp.). Geneva, Switzerland: World Meteorological Organization.
- Sevruk, B., & Klemm, S. (1989). *Catalogue of standard precipitation gauges*. Instruments and observing methods (WMO/TD No. 328, Vol. 39, 52 pp.). Geneva, Switzerland: World Meteorological Organization.
- Shroder, J. F., Bishop, M. P., Copland, L., & Sloan, V. F. (2000). Debris-covered glaciers and rock glaciers in the Nanga Parbat Himalaya, Pakistan. *Geografiska Annaler: Series A, Physical Geography*, 82(1), 17–31. <https://doi.org/10.1111/j.0435-3676.2000.00108.x>
- SIHP. (1997). *Snow and ice hydrology, Pakistan phase-II: Final report to CIDA* (Report No. 54, IDRC File No. 88-8009-00). Ottawa, Ontario, Canada: International Development Research Centre.
- Singh, P., & Kumar, N. (1997). Impact assessment of climate change on the hydrological response of a snow and glacier melt runoff dominated Himalayan river. *Journal of Hydrology*, 193(1–4), 316–350.
- Singh, P., Ramasastri, K. S., & Kumar, N. (1995). Topographical influence on precipitation distribution in different ranges of western Himalaya. *Nordic Hydrology*, 26, 259–284.
- Tahir, A. A., Chevallier, P., Arnaud, Y., & Ahmad, B. (2011). Snow cover dynamics and hydrological regime of the Hunza River basin, Karakoram range, northern Pakistan. *Hydrology and Earth System Sciences*, 15(7), 2275–2290.
- Tuinenburg, O., Hutjes, R. W. A., & Kabat, P. (2012). The fate of evaporated water from the Ganges basin. *Journal of Geophysical Research*, 117, 1–17. <https://doi.org/10.1029/2011JD016221>
- Voisin, N., Wood, A. W., & Lettenmaier, D. P. (2008). Evaluation of precipitation products for global hydrological prediction. *Journal of Hydrometeorology*, 9, 388–407.
- Wagnon, P., Linda, A., Arnaud, Y., Kumar, R., Sharma, P., Vincent, C., ... Chevallier, P. (2007). Four years of mass balance on Chhota Shigri glacier, Himachal Pradesh, India: A new benchmark glacier in the western Himalaya. *Journal of Glaciology*, 53(183), 603–611.
- Wake, C. P. (1989). Glaciochemical investigations as a tool for determining the spatial and seasonal variation of snow accumulation in the Central Karakoram, northern Pakistan. *Annals of Glaciology*, 13, 279–284.

- Water and Power Development Authority. (2003). *Annual report of river and climatological data of Pakistan, 2001* (Surface Water Hydrology Project, Vol. 2). Lahore, Pakistan: Hydrology and Water Management Organization.
- Water and Power Development Authority. (2012). *Annual report of river discharge, sediment and water quality data for the year 2010* (Surface Water Hydrology Project No. 71, Vol. 1). Lahore, Pakistan: Hydrology and Water Management Organization.
- Wei, J., Dirmeyer, P. A., Wisser, D., Bosilovich, M. G., & Mocko, D. M. (2013). Where does the irrigation water go? An estimate of the contribution of irrigation to precipitation using MERRA. *Journal of Hydrometeorology*, *14*, 275–289. <https://doi.org/10.1175/JHM-D-12-079.1>
- Winiger, M., Gumpert, M., & Yamout, H. (2005). Karakorum–Hindukush–western Himalaya: Assessing high-altitude water resources. *Hydrological Processes*, *19*(12), 2329–2338. <https://doi.org/10.1002/hyp.5887>
- Wolff, M. A., Isaksen, K., Petersen-Øverleir, A., Ødemark, K., & Reitan, T. (2015). Derivation of a new continuous adjustment function for correcting wind-induced loss of solid precipitation: Results of a Norwegian field study. *Hydrology and Earth System Sciences*, *19*(2), 951–967.
- Yang, D., Kane, D., Zhang, Z., Legates, D., & Goodison, B. (2005). Bias corrections of long-term (1973–2004) daily precipitation data over the northern regions. *Geophysical Research Letters*, *32*, L19501. <https://doi.org/10.1029/2005GL024057>
- Ye, B., Yang, D., Ding, Y., Han, T., & Koike, T. (2004). A bias-corrected precipitation climatology for China. *Journal of Hydrometeorology*, *5*(6), 1147–1160. <https://doi.org/10.1175/JHM-366.1>
- Yu, W., Yang, Y.-C., Savitsky, A., Alford, D., Brown, C., Wescot, J., ... Robinson, S. (2013). *The Indus basin of Pakistan: The impacts of climate risks on water and agriculture*. Washington, D.C.: The World Bank.

## SUPPORTING INFORMATION

Additional Supporting Information may be found online in the supporting information tab for this article.

**How to cite this article:** Dahri ZH, Moors E, Ludwig F, et al. Adjustment of measurement errors to reconcile precipitation distribution in the high-altitude Indus basin. *Int J Climatol*. 2018;1–19. <https://doi.org/10.1002/joc.5539>